ESDD PREDICTION OF OUTDOOR POLYMER INSULATORS

by

Abdelrahman Khaled

A Thesis Presented to the Faculty of the
American University of Sharjah
College of Engineering
in Partial Fulfillment
of the Requirements
for the Degree of

Master of Science in
Electrical Engineering

Sharjah, United Arab Emirates

June 2015

Approval Signatures

We, the undersigned, approve the Master's Thesis of Abdelrahman Khaled.

Thesis title: ESDD Prediction of Outdoor Polymer Insulators

Signature **Date of Signature** (dd/mm/yyyy)

_____ _____

Dr. Ayman Hassan El-Hag
Associate Professor, Department of Electrical Engineering
Thesis Advisor

_____ _____

Dr. Khaled Assaleh
Professor, Department of Electrical Engineering
Thesis Co-Advisor

_____ _____

Dr. Ahmed Osman-Ahmed
Associate Professor, Department of Electrical Engineering
Thesis Committee Member

_____ _____

Dr. Mohammad Jaradat
Associate Professor, Department of Mechanical Engineering
Thesis Committee Member

_____ _____

Dr. Nasser Qaddoumi
Interim Head, Department of Electrical Engineering

_____ _____

Dr. Mohamed El-Tarhuni
Associate Dean, College of Engineering

_____ _____

Dr. Leland Blank
Dean, College of Engineering

_____ _____

Dr. Khaled Assaleh
Director of Graduate Studies

Acknowledgments

First of all, I would like to thank Allah, the Most Gracious and the Most Merciful, for making this study possible. In addition, I would like to thank the cooperative people whose help also made this study possible. My acknowledgment goes to Dr. Ayman El-Hag for his understanding, patience, and motivation. Likewise, I would like to express my gratitude to Dr. Khaled Assaleh for his support and for co-advising this thesis. In addition, I would like to thank the Electrical Engineering Department at the American University of Sharjah for their continuous support and the teaching assistantship opportunity. Last but not least, I would like express my deep appreciation to my family and friends who gave me the moral support to keep going in my study.

Dedication

To those who work for

A better future…

Abstract

Reliable power transmission is a main factor in designing transmission and distribution lines. Contaminated environments significantly reduce the performance of outdoor insulators in which the accumulation of contamination eventually leads to a complete flashover. The main factors that lead to contamination flashover include, operating voltage, humidity level and temperature. Contamination flashover happens when soluble or non-soluble deposits cover the surface of the insulator, which results in a reduction of the surface resistance. The flashover event is the main problem that affects the life-time of the insulators reducing the security and reliability of the power transmission system. Controlling the risk of flashover is practically done by cleaning and replacing heavily polluted insulators. However, there is no standard technique for scheduling cleaning or maintenance of outdoor insulators, which in some cases can extend for hundreds of kilometers. To make this process as efficient as possible, many researchers are trying to develop techniques for flashover prediction. In the past, some researchers used the leakage current to predict the contamination level on the surface of ceramic and porcelain outdoor insulators. This can help as a mean to warn transmission power operators about the advent of contamination flashover. However, there have been few researches to predict the contamination levels on the surface of non-composite or polymer insulators. This work aims to develop a practical technique to monitor and evaluate the surface condition of non-composite by predicting the soluble contamination level. In this research, the leakage current was used to predict the soluble salt deposit on the surface of polymer insulators. Based on this prediction the surface condition of the insulator was evaluated.

Search Terms: *Outdoor Polymer Insulators, Leakage Current, ESDD Prediction, Contamination Flashover.*

Table of Contents

List of Figures

List of Tables

Abbreviations

LC	-	Leakage Current
ESDD	-	Equivalent Salt Deposit Density
NSDD	-	Non Soluble Density Deposit
PCA	-	Principle Component Analysis
KNN	-	K-Nearest Neighborhood
NN	-	Neural Network
ANFIS	-	Adaptive Neuro Fuzzy Inference System
NaCl	-	Sodium Chloride
RMSE	-	Root Mean Square Error

Chapter 1: Introduction

1.1 Problem Statement

High voltage outdoor insulation design and monitoring are vital to ensure reliable power transmission and distribution. Outdoor insulators have two main functions in overhead lines, which are providing electrical insulation to the conductor and providing mechanical support to the structure. In order to sustain their role in overhead lines, the outdoor insulators must be able to withstand different types of stresses including, electrical stresses, and mechanical loads under different environmental conditions. Ceramic insulators have been employed in the field since 1800 and they are characterized by great mechanical stability and long life time. On the other hand, polymer insulators were first introduced in 1959 and nowadays they are being increasingly used worldwide. The polymer insulators have certain advantages including light weight, low cost and superior contamination resistance as a result of their excellent hydrophobic properties [1].

The main concerns which arise for polymer insulators are their long term pollution performance and aging due to tracking and erosion. The process of aging in polymer insulators starts with the loss of hydrophobicity allowing the flow of leakage current, which causes further aging processes like dry-band arcing. The dry-band activities deteriorate the polymeric material and eventually bridge the whole length of insulator causing a flashover incident. Therefore, monitoring of leakage current is extremely essential to evaluate the aging condition of outdoor insulation. The leakage current magnitudes showed no correlation with the aging state of insulators. However, the leakage current shape [8] and frequency spectrum [9] can be used to monitor and assess the surface and aging conditions in insulators.

The leakage current development can be categorized into three stages: namely the early aging period, transition period and final aging period [14]. Leakage current measurement is used in lab tests in order to study the performance of outdoor insulators under different conditions as well as to study different aging mechanisms. Salt fog test is a standard test, which is used to study the flashover performance and aging mechanisms including, loss of hydrophobicity and dry-band arcing [1]. In addition, leakage current monitoring is widely used by power utilities in the field in order to examine the conditions of outdoor insulators.

Leakage current measurement is a very popular technique to monitor the pollution performance of outdoor insulators. Many researchers have used leakage current to predict the pollution severity on the surface of insulators and to predict the flashover voltage. The prediction of leakage current can give a good indication of the surface state of insulator which can be used to better plan an efficient cleaning and maintenance schedule. Cleaning routines for outdoor insulators is time consuming and very expensive as the transmission lines may extend for hundreds of kilometers. If leakage current monitoring is employed to predict early contamination levels, then the scheduling of cleaning and maintained can be optimized to minimize effort and money.

Environmental conditions have the greatest effect on the performance of the outdoor insulators. The accumulation of contamination, like salt, dust and sand eventually leads to a complete flashover on the surface of the insulator. Contamination flashover has become a significant aspect in designing outdoor insulators and it has been under extensive research. When the insulator surface gets covered by soluble salts and moisture, the insulator surface becomes more conductive. After the formation of conductive layers, dry band regions will appear on the surface leading to the start of partial arcs. These arcs get elongated which finally bridges the whole insulator leading to a flashover.

Many researches have been conducted to predict the contamination level on the outdoor insulators in order to prevent the advent of flashover occurrence. Knowing the contamination levels can serve as warning system and help in scheduling washing and maintenance routines. All researches were performed on ceramic, porcelain and glass insulators. The researchers found that the leakage current peak value is the most effective in the prediction of contamination levels along with the environmental conditions including, operating voltage, temperature and humidity.

However, to the best of our knowledge, no research has been done to predict the contamination level for polymer insulators. The main objective of this research is to use the leakage current parameters techniques in order to predict the soluble salt deposit (ESDD) level for polymer insulators. This can help in evaluating the surface condition of the insulator which will enhance the monitoring, cleaning and maintenance of insulation along the transmission lines.

1.2 Thesis Contribution

Previous researches have been conducted to correlate the ESDD and Leakage current for ceramic and porcelain outdoor insulators. Since polymer insulators are relatively new and their mechanism of suppressing the leakage current known as hydrophobicity is not fully understood, it is difficult to predict the ESDD level on its surface. Very few researches were performed to predict the contamination level on the surface of polymer outdoor insulators. In this study a practical approach is developed to evaluate the surface condition of polymer insulation by predicting the ESDD level on its surface. This work can help in developing a practical monitoring system for outdoor polymer insulator which will allow power system operators to schedule maintenance and cleaning routines based on practically more precise measures.

1.3 Thesis Arrangement

The next chapters of this thesis are arranged as the following. Chapter 2 provides a background on outdoor insulation, polymer insulator as well as leakage current monitoring and ESDD prediction. The literature review about the leakage current and ESDD prediction is provided in chapter 3. Chapter 4 explains the experimental setup, experimental procedure and the data collection. An overview of the pattern recognition techniques which will be used for the prediction of the ESDD Level is described in chapter 5. Then chapter 6 presents and discusses the main findings of this study. Finally, Chapter 7 will conclude this work and give recommendations for further work.

Chapter 2: Outdoor Insulators

2.1 Outdoor insulators

Outdoor insulators are essential elements in power distribution and transmission overhead lines. They are primarily required to support the outdoor conductors as well as to electrically insulate the conductors from the supporting structures. Most of the generated electric power is transmitted through overhead lines at high voltages (hundreds of kV) in order to minimize the power losses. The line voltage conductors operating at such high voltages need to be connected to the support structures, and they also need to be insulated. Both functions are performed by the outdoor insulators, which are expected to provide mechanical support and electrical insulation. Moreover, these insulators must also withstand the outdoor conditions that they are normally subjected to [1].

During their operation time, three types of stresses are encountered by outdoor insulators which are mechanical, electrical and environmental stresses. These stresses vary according to the application and surrounding conditions of the insulators. For instance, line posts can experience mechanical loads like cantilever or bending loads, while suspension insulators are subjected to tensile loads. In addition, wind and ice adds more mechanical load to the insulator. Some transient loads can also impact the insulator including vibrational loads, shock loads due to natural disasters or man-made actions like vandalism (gun shots).

The electrical stresses include steady state or normal operating voltages and frequencies. They also include transient voltages or voltage surges that result from switching and lightening events. These voltage surges impose a higher stress on the insulator but for shorter durations. The outdoor environmental conditions include temperature, which increases the conductivity of insulating materials. Ultraviolet radiations may cause breakdown or cross linking of certain chemical bonds leading to surface degradation. Contamination resulting from rain, dew, fog, ice or moisture in general decreases the surface resistance of insulators. Therefore, the outdoor insulators must be designed to withstand steady state and transient stresses whether they are electrical or mechanical under different environmental conditions.

One of the earliest, yet most significant challenges faced by insulator designers is the environmental effects on their performance. Contaminated

environments have a great effect in reducing the performance of outdoor insulators in which the accumulation of contamination eventually leads to a complete flashover. Contamination flashover has become the most significant aspect in designing outdoor insulation and hence it needs to be carefully studied [2].

For contamination flashover to occur, the insulator surface needs to be covered with soluble salts and moisture which are generally referred to as pollution. Moisture plays a critical role in the flashover process because under dry conditions, the contaminants are non-conducting. Therefore, light rain, fog and mist are very dangerous to outdoor insulators as they wet the surface making the pollution layer conductive. After the formation of conductive layers, dry band regions will appear on the surface leading to the start of partial arcs. These arcs get elongated which finally bridges the whole insulator leading to a flashover.

There are two main categories of outdoor insulators which are ceramic and polymer insulators. The ceramic insulation is normally made of two materials, either porcelain or glass. Polymer insulators are made of composite material and generally comprise a fiber glass core protected by rubber housing. The polymer insulators were introduced due to their, light weight, contamination resistance, vandalism resistance, low cost and easier handling. However, composite insulators are subjected to long term aging processes leading to the deterioration of their mechanical and electrical properties. The ceramic insulators on the other hand are more chemically and mechanically stable. However, they have low pollution resistance, heavy weight and are more expensive.

2.2 Polymer Outdoor Insulation

2.2.1 Structure of Polymer Insulation

The first polymeric outdoor insulators can be traced back to 1959 and they were made of epoxy. However, they failed when applied to outdoor contaminated conditions. The modes of failure were due to ultraviolet degradation, tracking and erosion. The sixties and seventies experienced an increase in the production of polymer insulators. These insulators had the same fundamental design features as the contemporary designs as illustrated in Figure 1. A fiber glass rod was used as the core material to give the necessary support, while the rubber housing provided protection from the environmental conditions and contaminations [2].

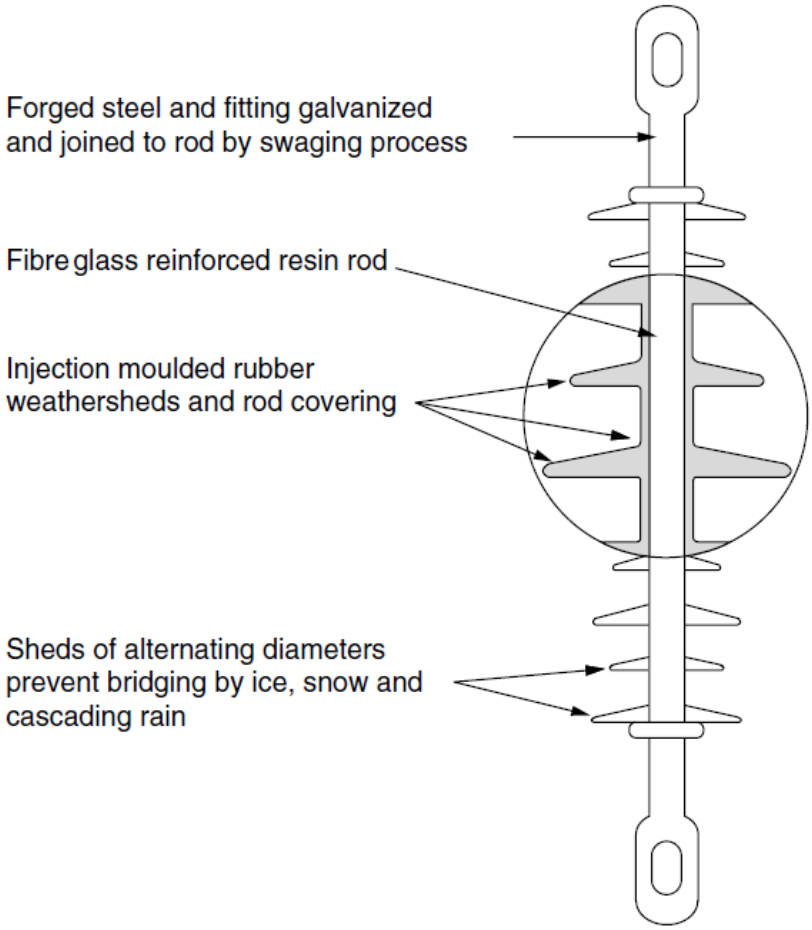

Figure 1: Structure of Composite Insulators [2]

Typically a composite insulator comprises a core material, end-fitting, and a rubber insulating housing. The core of the insulator is made from fiber-reinforced plastic (FRP) to distribute the tensile load providing mechanical support to the insulator. The reinforcing fibers used in FRP are glass (E or ECR) and epoxy resin. The sheath of the insulator is made from silicone rubber which provides electrical insulation and weather resistance. The weather resistance is essential to protect the insulator's core from environmental conditions. The silicone rubber is particularly famous for its excellent hydrophobic properties, which has a great effect in resisting the contamination conditions and aging processes encountered by the insulator during its service time.

2.2.2 Hydrophobic Properties of Polymer Insulation

One of the greatest advantages of polymeric insulators over ceramic insulators is its ability to resist the formation of continuous water films above its surface, suppressing leakage currents (LC), dry-band arcing and flashover. This surface

property is known as hydrophobicity, and is defined as the ability of the insulator to repel water on its surface, forming individual droplets rather than a film [3]. The hydrophobic behavior of polymer insulators arises due to the low surface energy on its surface. Hydrophilic materials, like ceramic insulators, have higher surface energy allowing the formation of water films on its surface [4]. The hydrophobic properties of polymer insulators have been widely investigated to understand the surface condition of insulators. Figure 2 shows the leakage current development in both ceramic and polymer insulators.

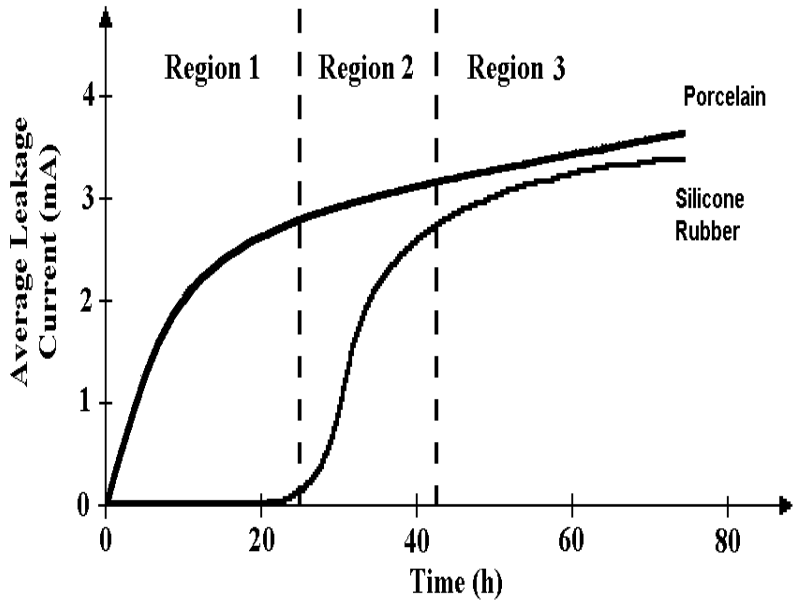

Figure 2: Leakage Current Development in Porcelain and Rubber Insulators [7]

As depicted in Figure 2, the leakage current development in porcelain is very fast compared to silicone rubber. The hydrophobic behavior of silicone rubber suppressed the leakage current formation for much longer time. The hydrophobicity is commonly evaluated by measuring the static contact angle between the water droplet and the surface. Other methods like dynamic contact angle, Swedish transmission research institute, sliding angle and water soaking can also be used to quantify hydrophobicity [3]. The contact angle for hydrophobic surfaces is higher compared to hydrophobic surfaces as shown in Figure 3,

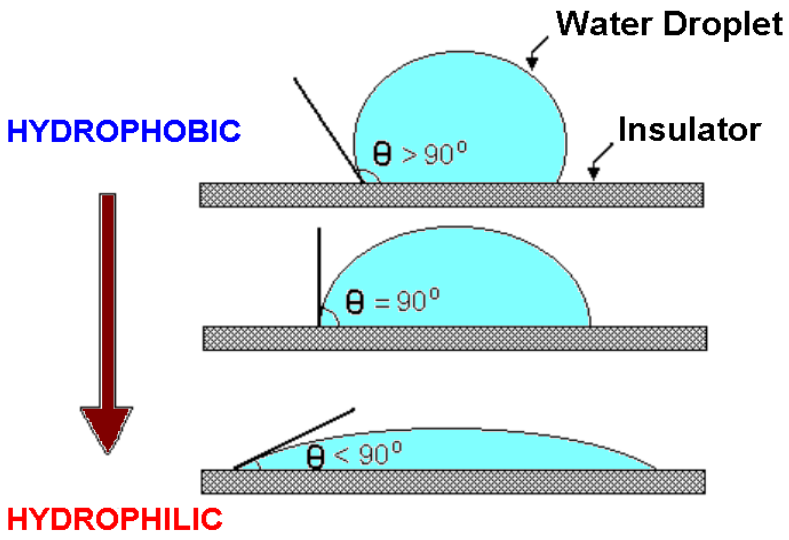

Figure 3: Relation between Contact angle and Hydrophobicity [34]

The hydrophobicity of silicone rubber is lost due to chemical reactions on the surface. For instance corona discharges result in oxidation reactions, which lead to the decrease in hydrophobic properties. Other reasons for the loss of hydrophobicity include, surface pollution, UV radiations and temperature. However, after the removal of the electric or environmental stresses, the polymeric insulators can recover the hydrophobic properties again. The most significant process for the hydrophobicity recovery is the migration of the low molecular chain fluids from the bulk of the material to the surface of the silicone rubber [5]. The process of loss and recovery of hydrophobicity occurs several times during the life time of silicone rubber insulators.

2.3 Aging Process in Polymer Insulators

Unlike porcelain and glass insulators, the flashover events in composite insulators are much less frequent. The excellent water repellency property of silicone rubber suppresses the formation of leakage current, which in turn reduces the possibility of flashover. The causes of failure in polymer insulators are largely mechanical in nature [3]. As a result of housing damage, the fiber glass core gets exposed to the outdoor conditions, which can cause brittle fraction of the core. The aging process starts with the loss of hydrophobicity which leads to the development of leakage currents and eventually to dry-band arcing which causes a deterioration to the insulator material [6].

The main cause for initiating the aging process in polymer insulators is the development of corona discharges [3]. When the surface of insulator is contaminated with water droplets, the electric field gets enhanced at the triplet point between, the air, water molecule and the insulator surface. Figure 4 shows the field enhancement, around the triplet point, due to the presence of a single water droplet on the surface of silicone rubber insulator. This field enhancement causes the development of small partial discharges known as corona, which attack the surface of insulator leading to chemical changes. Although the energy associated with the partial discharges are very weak, however; their high frequency occurrence can lead to a temporary loss of hydrophobicity [7].

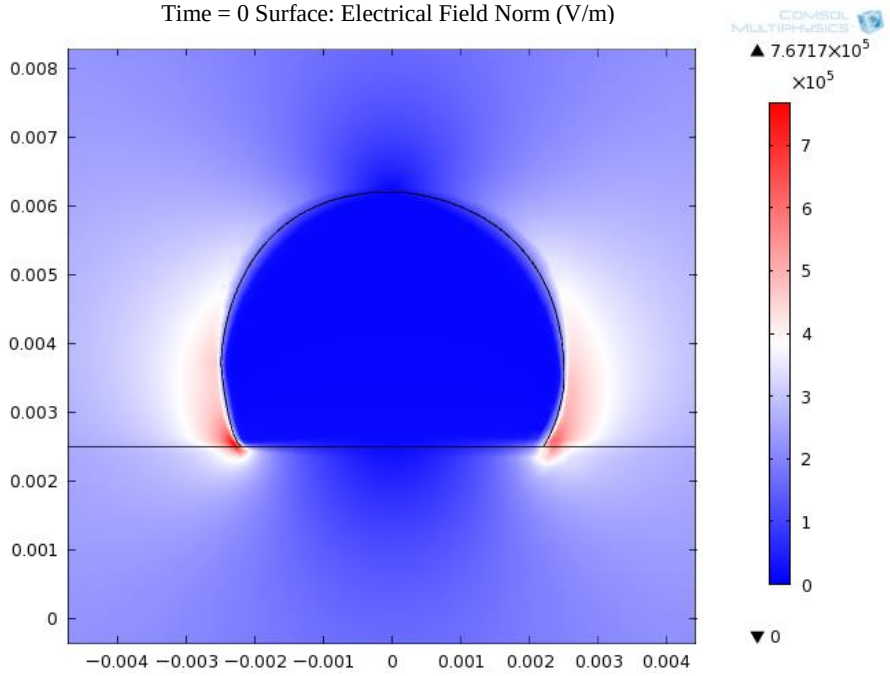

Figure 4: Field Enhancement due to Water Droplet

As the surface of insulator becomes hydrophilic, water droplets start to be converted into continuous filaments, leading to the development of leakage currents, which heats up the insulator surface. However, the current density on the surface is non-uniform, and hence the heat dissipation in some regions is much higher than other regions, leading to water evaporation. This non-uniform water evaporation forms narrow dry bands on the surface, which changes the voltage distribution and causes greater discharges, known as dry-band arcs, to bridge the dry bands [7].

There are three aging periods, through which the development of leakage current takes place, which are: early aging period, transition period and final aging period. The leakage current normally follows a pattern as shown in the Figure 5,

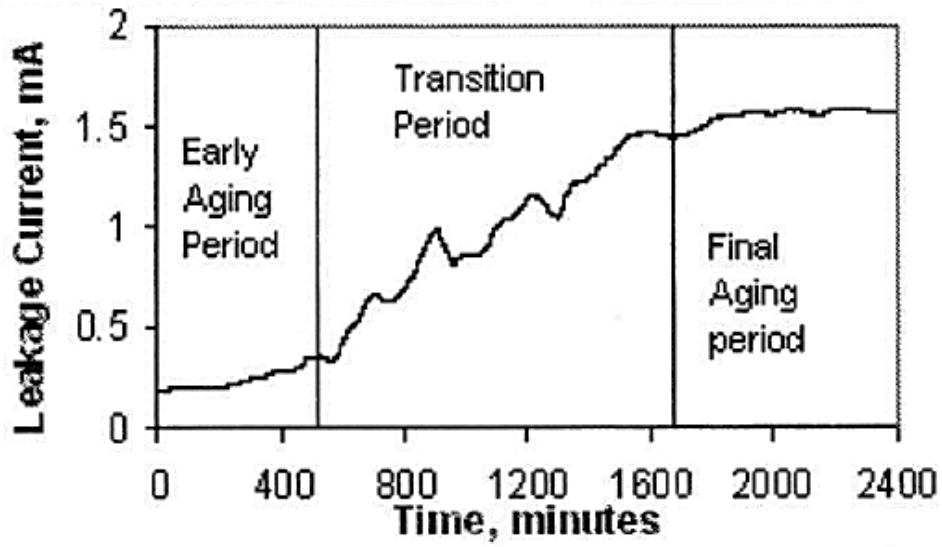

Figure 5: Aging Process for Composite Insulators [21]

In region one, early aging, the insulator's surface hydrophobicity is still preserved, suppressing the leakage current development, while the migration of low molecular weight fluids to the surface helps to maintain the hydrophobicity property. In region two, transition period, the insulator surface becomes wet, as a result of partial loss of hydrophobicity, while dry band-arcing starts to develop at this stage. In the last stage of aging, the hydrophobic properties are completely lost and the leakage current reaches a saturation level, where the dry-band arcing starts to degrade the material [7].

2.3.1 Leakage Current Characteristics

The leakage current is one of the most important parameters to assess the performance of outdoor insulators. The magnitude of leakage current can be related to the contamination level on the insulator surface. However, the studies have shown no correlation between the leakage current magnitudes and the aging state of polymer insulators [8]. The shape of the leakage current signal [8] and its frequency spectrum [9], on the other hand; can give information about the surface conditions of the insulator. For instance, when the hydrophobicity is still maintained the leakage current is capacitive, however; hydrophilic surfaces are characterized by resistive leakage currents [7] as shown in Figure 6,

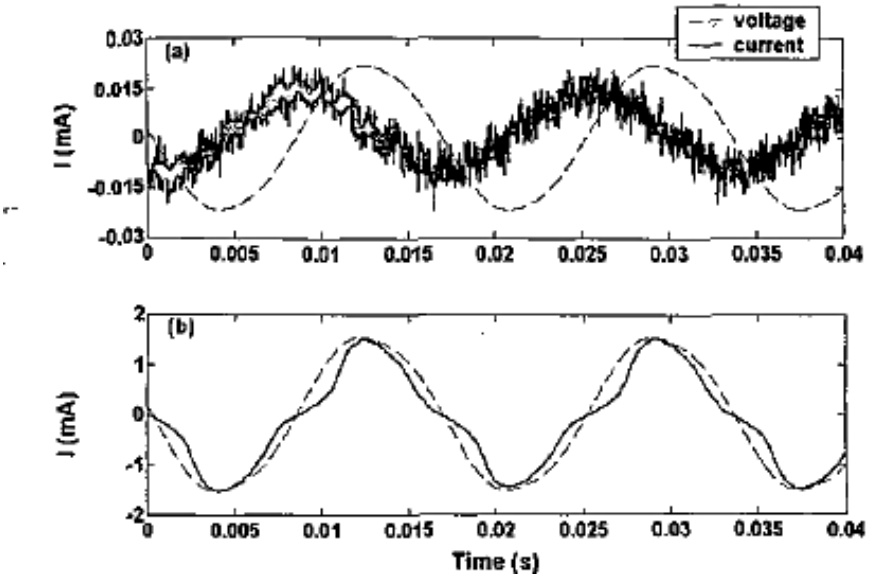

Figure 6: (a) Capacitive LC (Hydrophobic) and (b) Resistive LC (Hydrophilic) [7]

In Figure 6(a), it can be noticed that the leakage current is capacitive since the phase shift between the leakage current and applied voltage is almost 90 degrees. However, in Figure 6(b), the leakage current is in phase with the applied voltage indicating a resistive leakage current. Moreover, the harmonic content of leakage current, specifically the odd harmonics, were found to correlate well with the aging state of the insulator [10].

Different aging stages impose changes on the shape of leakage current waveforms. Figure 7 shows typical leakage current waveforms along with their frequency spectrum for different aging states of polymeric insulators. As mentioned earlier capacitive leakage currents follow through the insulation surface, as long as the hydrophobicity property is maintained. The leakage current in this condition is capacitive, sinusoidal with very low magnitudes, Figure 7(a). As the hydrophobicity is lost, more current flows and the phase shift between the leakage current and applied voltage starts to decrease. The current waveform, in this condition is still sinusoidal but resistive, while the magnitude of the leakage current is higher compared to the first condition as depicted in Figure 7(b). When dry-band activities start to take place, as a result of partial or complete loss of hydrophobicity, the leakage current pattern becomes resistive and non-linear. The magnitudes of such currents are also higher than the first waveform. Strong dry-band discharges can cause long spikes to appear on the leakage current signal as shown in Figure 7(c) [7].

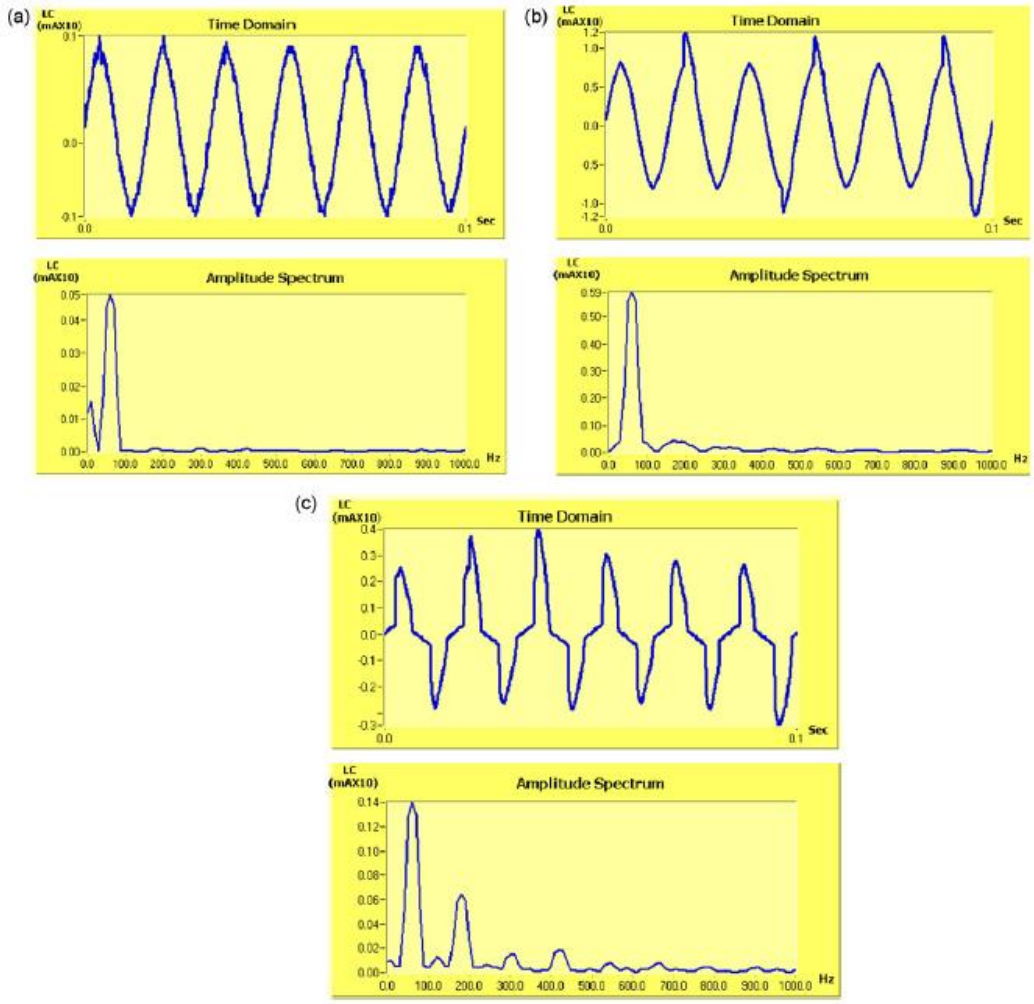

Figure 7: Time and Frequency LC signals during (a) early, (b) transition and (c) late aging period [14]

Observing the frequency spectrum of the leakage current, it can be noted that the fundamental components are the only significant portion of the frequency characteristics during early aging. As the resistive currents starts to develop, the 3rd harmonics will have the highest intensity among other harmonic components. When local arcs start to appear, other odd harmonics will grow rapidly and become more significant [9]. The leakage currents low frequency harmonics were found to correlate with the aging condition of insulator [10]. It was shown that the 3rd and 5th harmonics had a higher rate of increase compared to the fundamental component during dry-band arcing. However, with increased degradation due to erosion and tracking these harmonic contents were found to decrease, while the fundamental component started to increases. Therefore, the 3rd and 5th harmonic content can indicate the start of dry-band arcing and the start of tracking and erosion.

2.4 Leakage Current Monitoring

Polymeric insulators performance is largely affected by the aging processes which arise due to electrical and environmental conditions. Humid conditions resulting from fog, rain or mist accompanied by salt contaminants produce corona discharge, which degrades the surface hydrophobicity. The loss of hydrophobic properties initiates the development of leakage current which in turn causes more degradation processes such as dry-band arcing and even complete flashover. The leakage current frequency content can provide information about these degrading discharges and therefore; it has been used to evaluate the aging condition of outdoor insulators under both laboratory and field conditions [11].

The leakage current is measured under different aging tests in order to understand the aging process of outdoor insulators and correlate the findings to actual field conditions. In addition, it can be used to find the effect of different electrical and environmental stresses on the aging process and flashover performance. Particularly leakage current can be used in laboratory tests to study aging phenomena like corona discharges, hydrophobicity loss and dry-band arcing. There are different types of aging and flashover tests including salt-fog, clean-fog and inclined plane tests. The salt and clean fog tests are used for flashover testing and to study the effect of contamination level on the aging process, including corona and dry-band arcing. They are also used to evaluate tracking and erosion resistance. The inclined plane test is a classical method for evaluating the erosion and tracking resistance of outdoor insulators [12].

The salt fog test was developed to simulate the effect of wetting resulting from salty ocean water in coastal areas. It is used extensively in European countries and Japan. Under this test, a clean insulator is energized at a constant voltage while subjected to a salt-water nozzle. The test conditions severity is controlled by either changing the applied voltage or the concentration of sodium chloride in the water. The test was initially used to evaluate the flashover voltage under different contamination levels. However, wetting by water impingement is a very rare type of wetting [1-2]. Another method of generating fog is using ultrasonic humidifiers instead of the spray nozzles. The humidifiers generates a uniform fog, which produces a more uniform wetting and represents the majority of wetting instances in real conditions.

2.5 ESDD Prediction

2.5.1 Contamination Flashover and ESDD Prediction

Contamination flashover, as discussed earlier is the major problem in deteriorating the surface conditions of polymer insulators. The contamination problem has a direct impact on the security and reliability of the power transmission systems and therefore it needs to be fully understood. There are two main types of contamination which are:

1) Soluble Salt Deposit (ESDD)

2) Non-soluble Material Deposit (NSDD) like dust and sand

The accumulation of both soluble and non-soluble deposits increases the conductivity of the insulator surface allowing more current to flow. The increase in the leakage triggers the aging process on the insulator surface which eventually leads to flashover. The relationship between the ESDD level and the contamination classification according to the IEC 60587 standard is shown in Table 1 [33].

Table 1: IEC 605087 Standard Contamination Severity Classification

IEC 60587 Classification of Contamination Severity

ESDD Range (mg/cm^2)	Contamination Severity Classification
0 – 0.03	Clean or very light
0.03 – 0.06	Light
0.06 – 0.1	Moderate
>0.1	Heavy

In the few past years, there has been an increasing demand to predict the contamination level on the outdoor insulators in order to prevent the advent of flashover occurrence. The prediction of contamination levels can signal an early warning to power station operators and help in scheduling washing and maintenance routines. The exact parameters for determining the contamination level are not fully established. Several studies have been conducted to predict the contamination levels for ceramic, porcelain, glass and polymer [27-32] insulators. It has been found that the leakage current characteristics are very useful in the prediction of the contamination

levels [31]. In addition, there are other factors which dynamically affect both, the leakage current and contamination levels including, the operating voltage, temperature and humidity [29].

In most of the conducted studies, the insulators were first polluted with a known ESDD value, and then the insulator will be subjected to a high voltage stress and clean-fog. After the end of the experiment, the leakage current will be used to predict the applied ESDD level. However, in this study, salt-fog test will be applied to the insulator and then the ESDD level will be measured at the end of the experiment. The ESDD can be measured by cleaning the insulator with distilled water and then measuring the conductivity of the resulting solution. The details of ESDD measured are explained in the IEEE standard 4-1995 as discussed in the following section.

2.5.2 ESDD Calculation Procedure

According to IEEE Std. 4-1995, The ESDD should be collected from the surface of insulator by the following procedure [18]:

1. The salt deposit is collected from the surface of the tested insulator excluding metal parts and assembly materials.
2. A known quantity of distilled water with known conductivity is then used to wash the insulator surface and dissolve the salt deposit.
3. The ESDD is calculated by measuring the conductivity of the resulting water solution.

Then the ESDD is calculated by applying the following equations:

1. The layer conductivity at 20 degrees is first calculated as shown below:

$$\sigma_{20} = \sigma_{\theta}\,[1 - b(\theta - 20)] \quad (1)$$

where,

σ_{20} represents the layer conductivity at a temperature of 20 ^{0}C (S/m)

σ_{θ} represents the volume conductivity at a temperature of ^{0}C (S/m)

θ represents the temperature of the insulator surface (^{0}C)

b is a factor which depends on the temperature as shown in Table 2:

Table 2: Temperature Conversion for ESDD Claculation

Temperature θ	B
5	0.03156
10	0.02817
20	0.02277
30	0.01905

2. The salinity, S_a (kg/m^3) is then calculated by:

$$S_a = (5.7\ \sigma_{20})^{1.03} \quad (2)$$

3. Finally the Salt Deposit Density (mg/cm^2) is calculated as shown:

$$ESDD = \frac{Sa\,V}{A} \quad (3)$$

where,

V represents the volume of slurry (cm^3)

A represents the area of cleaned surface (cm^2)

Chapter 3: Literature Review

3.1 Leakage Current Prediction

The leakage current has been used to study the aging state of outdoor insulators. In particular the leakage current harmonics were found to correlate with dry-band arcing and hence with erosion and tracking [10]. In addition, the leakage current low harmonics were found to correlate with some weathering conditions, like humidity levels [11], and ultraviolet radiations [20]. The saturation level of leakage current during the early aging period was predicted for polymer insulators in [22]. In this study the experiment was performed for 100 hours and the saturation level for LC was recorded and predicted using neural networks. The features used in this study included the initial leakage current value and the rate of change of leakage current for the first 5 hours of the experiment. The accuracy for this experiment was 95 % when the training and testing was done on the same insulator rating. When the training and testing was done on insulators with different ratings, the accuracy was 81%.

3.2 Flashover Prediction

Flash over prediction was carried out in several studies [13-15].The time to flashover was estimated in [16]. The flashover performance of outdoor insulators has also been investigated using leakage current [17, 19]. In [23], the flashover time was predicted for ice covered polymer insulator using neural networks. The features used in this study included the phase difference, amplitude of 3^{rd} harmonic, amplitude of 5^{th} harmonic and leakage current envelope. The establishment of white arcs which lead to the development of flashover was predicted within a time frame of 1 to 36 minutes.

In [24], the flashover voltage was predicted for ceramic insulators. The features used in this study included the height, diameter, total leakage length, number of sheds and number of chain of the insulator as well as the surface conductivity. The prediction was performed using least square support vector machine with a Root mean Square Error (RMSE error) of 0.00812 and multilayer feed-forward neural network with an RMSE error of 0.0126.

In [25], the flashover voltage was predicted for polymer insulators using neural networks. The features used included, water conductivity, number of water droplets and volume of water droplets. The accuracy for this prediction was 96%. In

[26], the flashover voltage was predicted for porcelain insulators using back propagation neural networks. The features used included, height, diameter and creepage distance of the insulator as well as the form Factor and the surface conductivity. The flashover voltage was predicted with an RMSE value of 0.112.

3.3 ESDD Prediction

The ESDD prediction has been carried on ceramic and porcelain insulators [27-31]. However, few researches have been done to predict the contamination level for polymer insulators [32]. The main concern for polymer insulators is the hydrophobic properties which have a great influence in the development and suppression of leakage current and on the contamination level on the insulator's surface. This concern arises as the hydrophobic properties of the polymer insulation are not fully understood. In addition, there is no established or practical technique to monitor and measure the hydrophobic properties of polymers for long durations. This limitation may affect the accuracy of ESDD prediction, however; it is still possible to make practical classification of the ESDD levels on polymer insulators as presented in this research.

In [27] the ESDD was predicted for porcelain insulators by processing the image of the contaminated insulators. Fifty one porcelain insulators were collected and their ESDD levels were measured. The ESDD levels were classified into 4 classes as shown in Table 3. The insulators image was processed and compared against an image of a clean insulator to predict the ESDD level. The percentage difference between the hue histograms of clean insulator reference image and polluted insulator image is calculated using six features including, the normalized error, mean, variance, skewness, kurtosis and energy. The feature extraction was done using hue segmented image technique and the prediction was done using a neural network. Thirty six insulators were used for testing and fifteen insulators were used for testing. The ESDD was predicted with an RMSE value of 0.0407. Furthermore, the class of the ESDD was predicted with an overall recognition of 86.7 % as shown in Table 3.

The overall recognition rate for this study is high, around 87%. However, the recognition rate for classes B and C are low, 50% each. The reason for this low recognition rate is the small number of available class B and C data.

Table 3: ESDD levels and classification results

ESDD Class	ESDD Range	Number of Data Points	Recognition Rate
A	< 0.1	8	100%
B	0.1 – 0.2	2	50%
C	0.2 – 0.3	2	50%
D	> 0.3	3	100%
Total		**15**	**86.7%**

In [28], the ESDD was predicted for glass disk insulators using neural networks. The glass disk insulator samples were pulverized by 5 pollution levels according to the IEC 507 standard. The five pollution levels as well as a clean insulator were used to create 6 classes as shown in Table 4.

Table 4: ESDD Classes

ESDD Class	ESDD Range mg/cm^2
A	0.00
B	0.000 - 0.032
C	0.032 - 0.038
D	0.038 - 0.056
E	0.056 - 0.123
F	> 0.123

The insulators were subjected to a clean fog test and the surface discharges acoustic signals were collected using an ultrasonic sensor. The Area centroid feature extraction technique was applied to the ultrasonic signals to predict the applied ESDD class. The classification was done using neural networks and the recognition rate was 95%.

In [29], the ESDD level was predicted for porcelain insulators using neural networks. The insulators were polluted by 9 ESDD values, which are 0.017, 0.04, 0.07, 0.09, 0.13, 0.25, 0.28, 0.34 and 0.37 mg/cm^2. Clean fog test was applied at different humidity and temperature levels. The humidity level ranged from 70% to 100% and the temperature ranged from 5 to 27 degrees. The leakage current was used to predict the applied ESDD level. The LC features used are the maximum leakage

current and 3rd harmonic to fundamental ratio. In addition, the applied humidity and temperature were also used as features. The ESDD prediction was carried using neural networks and the accuracy rate was 92%.

In [30], the ESDD level was predicted at the surface of contaminated glass plates using neural networks. The surface of the glass plates was polluted with NaCl solution and dried for 60 seconds. The dry salt granules were collected from the surface and mixed with distilled water to find the ESDD level at the surface. The experiment is repeated for 42 times using NaCl solutions of different conductivity and different plate sizes. The measured ESDD level ranges from 0.013 to 0.168 mg/cm^2. The features used to predict the ESDD included the temperature, salinity of the salt solution, the volume conductivity, the volume conductivity at 20^0 C, salt quantity, type of water and the plate size. Thirty seven data points were used for training and seven data points were used for testing. Back propagation neural networks were used to predict the ESDD level with an R^2 value of 0.981.

In [31], the ESDD level was predicted for porcelain insulators using neural networks. Clean fog test was applied to 2 porcelain insulators of different length at 20.2 kV and 100 % relative humidity. The pollution level was adjusted by applying a contamination layer of 5 different ESDD levels (0.03, 0.05, 0.1, 0. 2 and 0.3 mg/cm^2). These five ESDD levels were applied to each insulator resulting into 10 experimental values. The experiment was performed for 20 minutes. The leakage current mean, maximum value and standard deviation were used as the feature vector. For each insulator 50 data points were used for training and 10 data points were used for testing. The ESDD was predicted using neural networks with an absolute difference of 0.035 mg/cm^2.

In [32], the ESDD level was predicted for polymer insulators using neural networks and neuro-fuzzy inference system (ANFIS). Clean fog test was applied to a polymer insulator at 11 kV and 100 % relative humidity. The pollution level was adjusted by applying a contamination layer of NaCl and Kaolin of 5 different ESDD levels (0.01, 0.06, 0.08, 0.12 and 0.25 mg/cm^2). The experiment was done once for each ESDD level. The leakage current mean, maximum value, standard deviation and total harmonic distortion were used as the feature vector. 50 leakage current signals were recoded for each ESDD level resulting into 250 LC data points. 180 data points were used for testing, 40 for validation and 30 for testing. The LC characteristics were used to predict the applied ESDD level. The neural network predicted the ESDD with

an RMSE error of 0.0252 and the ANFIS system predicted the ESDD with an RMSE error of 0.00323.

For most of the studies discussed in the section for ESDD prediction, the following limitations can be noted. First, there are very few studies performed to predict the ESDD level for polymer insulators. Second, the number of predicted ESDD levels is very small. For instance, in studies [28], [31] and [32] only 5 ESDD levels were applied and predicted. In study [29] 9 ESDD levels are applied and predicted. Third, the experimental duration is usually small with a maximum of 20 min duration. To enhance the practicality of the experiments, in this study salt fog test was applied for polymer insulators for 5 hours duration. At the end of the experiment, the insulators were washed and the ESDD level deposited on the insulator's surface was measured according to the IEEE standard. The experiment was repeated to produce 80 different ESDD levels. The leakage current was recorded and used to predict the ESDD level which deposited on the surface of the insulator.

Chapter 4: Materials and Methods

4.1 Salt-Fog Aging Test

Salt fog test will be used as an aging test to predict the level of salt deposition on the surface of the insulator. The fog is generated using an ultrasonic humidifier with a maximum flow rate of 0.3 l/min. The rate of flow can be adjusted to change the humidity level, which is measured using a humidity sensor. The experiment is done at different voltage levels and water conductivities. The water conductivity is adjusted by changing the concentration of added NaCl, and is measured by a conductivity meter. At the end of the experiment each insulator was washed by distilled water to collect the salt deposition on the surface. The ESDD level is calculated by measuring the conductivity level of the water.

4.2 Experimental Procedure

4.2.1 Experimental Setup

The fog chamber used has a dimensions of 1x1x0.75 m, where the insulators are energized by a 0.22/20 kV transformer. The other end of the insulators will are grounded using a 100 ohm resistor. The leakage current is determined by measuring the voltage drop across the shunt resistance. Before measurement, the voltage was stepped down by a factor of 1000 using a voltage divider with ratio 1000:1. The protection circuit is designed in parallel with the grounding resistance. It consists of a surge arrestor to protect the system from transients and it also has a clipping circuit to limit the voltage between -9 and 9 V in order to protect the measuring devices [33]. Figures 8 and 9 show the fog chamber schematic, and the actual fog chamber setup respectively. In order to acquire more test data, four similar insulators will be tested simultaneously.

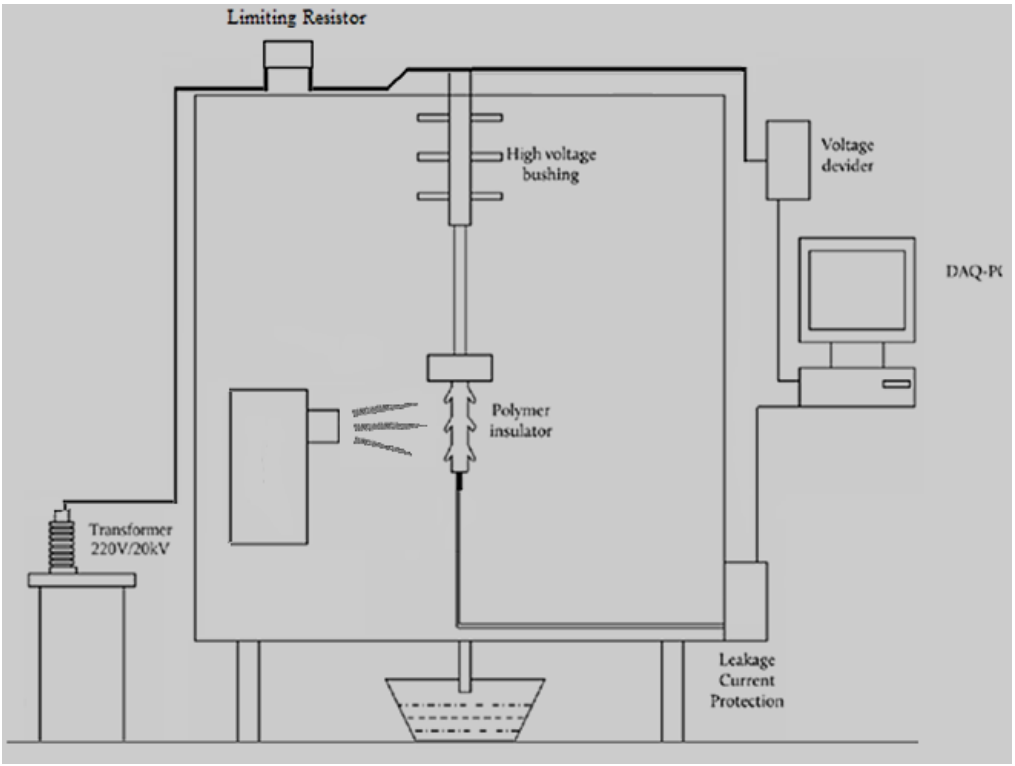

Figure 8: Fog Chamber Schematic [34]

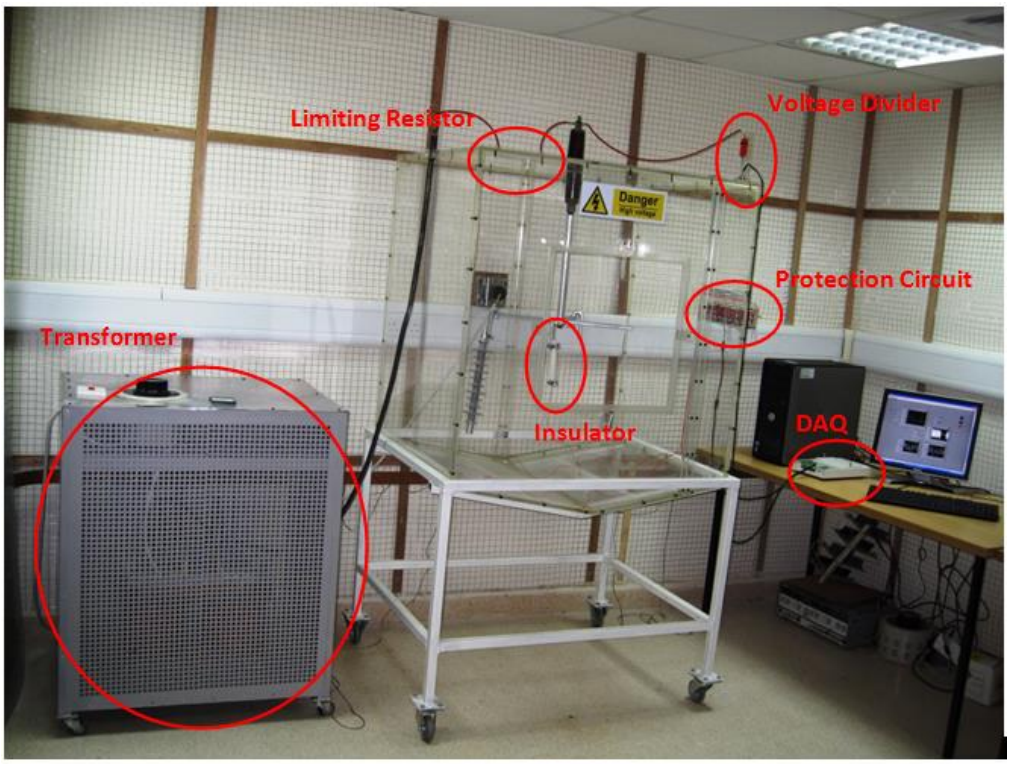

Figure 9: Fog Chamber Setup [34]

4.2.2 Experimental Test Procedure

The duration of each experiment is fixed to 5 hours. All insulator samples have the same type, where two sets of insulators were used. The first set consists of 4 insulators which have a length of 6 cm each, while the second set consists of 4 insulators which have a length of 10 cm each. Different factors have been varied during the salt fog test. These factors are:

1. Voltage Stress
2. Salt-fog conductivity
3. Insulator length expressed

Table 5 shows the ranges for each of the experimental factors:

Table 5: Experimental Conditions

Factor	Unit	Range
1. Electric Field	kV/cm	0.1 – 0.6
2. Salt-fog conductivity	S/cm	10, 15 and 20
3. Insulator length	cm	6 and 10

The Experiment was repeated for 20 times at different voltage stress, salt-fog conductivity and insulator length.

4.3 Data Collection and Feature Selection

4.3.1 Data Collection

The data was collected using a data acquisition system and it was processed using Labview interface. The applied voltage level and leakage current are measured each 10 seconds during the whole duration of the experiment. Therefore, the feature vector for the leakage current and voltage level has a total of 1800 points. The leakage current was smoothed using moving average technique [22]. The full leakage current waveform is not collected; however, the following features of the leakage current are measured and saved:

1. Peak Value
2. Fundamental Component
3. Third harmonic

These features will be used later to predict the ESDD level.

4.3.2 Feature Selection

In order to predict the ESDD, the most relevant features are selected. Possible features for prediction include LC peak value, slope of the leakage current, fundamental, third and the fifth harmonic components of leakage current. A combination of these features was created using pattern recognition techniques, including stepwise regression and principle component analysis. In addition, the experimental conditions including voltage, salt-fog conductivity and insulator length will be used in the feature vector as they have a direct effect on the salt level deposition.

4.4 Feature Extraction and Classification Techniques

The following chapter gives a background on the feature extraction techniques as well as the classifiers which will be used in the results analysis. Two feature extraction methods will be used and compared, which are:

1. Stepwise Regression
2. Principle Component Analysis (PCA)

In addition, three classifiers will be used in this study including:

1. K-Nearest Neighbor Classifier (KNN)
2. Polynomial Classifier
3. Neuro-fuzzy Classifier

The following section will provide an overview of the pattern recognition principles with regard to the feature extraction and classification process. Afterwards, the feature extraction methods and classification techniques will be discussed.

4.4.1 Pattern Recognition Review

Pattern recognition is defined as the process in which the inputs are assigned with labels. Depending on the type of problem, the assigned labels may be a distinct group, which is commonly known as a class. In that case, the goal of the pattern recognition system or "classifier" is to identify the correct class of each input in a process known as classification [35]. However, if the labels are real-value then the pattern recognition process or "regression", tries to find the exact value for each input. The pattern recognition process has several steps starting with data collection, data pre-processing, feature extraction and classifier design, training and testing as shown in Figure 10.

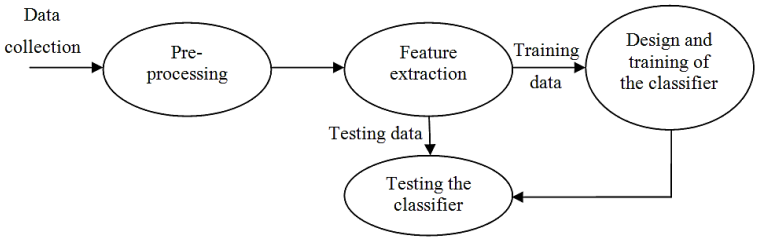

Figure 10: Pattern recognition steps [36]

During the data collection, the raw data are collected for certain conditions which correspond to a specific output. The output could be a class of data or a real-value data depending on the problem being studied. During the second stage, data pre-processing, the raw data is converted into a meaningful data input which could be done by statistical representation like the mean, standard deviation or by taking the Fourier transform or other data processing techniques.

During feature extraction the most distinguished features are being selected, which will help the classifier to accurately represent the data and predict the correct output. The feature extraction process depends on the knowledge of the factors which affect the required outcome. It has been reported that the main factors which correlate with the ESDD level include [29-30]:

1. Applied Voltage Stress.
2. Creepage Distance of insulator.
3. Environmental Conditions, like humidity and temperature.
4. Leakage Current.

Therefore, these factors will be used as features to predict the ESDD level. If the number of features is very large, then the dimensionality of the feature vector can be reduced by the feature extraction methods mentioned earlier.

The classifier design largely depends on the distribution shape of the data. Linear relationships can be easily modeled using linear classifiers, while quadratic relationships can be modeled using polynomial classifiers. Gaussian distributions are modeled by Gaussian Naive Bayes Classifier. If the distribution of data is unknown, then different classifiers can be used, starting with simple classifiers like linear, polynomial and KNN classifiers. If these classifiers don’t produce good recognition rates, then more advanced classifiers can be used, like Neural Networks and Neuro-fuzzy classifiers. The experimental data to be classified is sorted into two data sets,

the training data and testing data. The training data is used to design the classifier parameters, while the testing data is used to validate the design.

4.4.2 Feature Reduction Techniques.

4.4.2.1 Stepwise Regression.

The stepwise regression technique aims to find the best subset of features by searching for different feature combinations. The method works by adding or deleting the features which have the greatest impact on the residual sum of squares (RSS) [37]. The residual sum of squares represents the summation of the square difference between the predicted value and the mean value as shown below:

$$RSS = \sum_{i=1}^{n} \left(y_i - f(x_i)\right)^2 \quad (4)$$

There are two main selection criteria which are forward selection and backward elimination. In the forward selection, the stepwise starts with no features. Each feature is added separately and its effect on the model is noted. The feature which produces least residual sum of squares is chosen as the first feature. Other feature combination will be added until there is no improvement on the model. The backward elimination method starts with all features, and then the effect of deleting features is noted. The algorithm deletes the features which best improve the model by being deleted [41].

4.4.2.2 Principle Component Analysis (PCA)

The Principle Component Analysis, known as the Karhunen-Lo`eve expansion is a well-known reduction technique, that combines an old feature vector **x** to produce a new feature vector y. The PCA feature reduction preserves all necessary information which is required for the classification. The PCA technique works by projecting the old feature vector into the direction of the largest variance. In that sense, the dimensionality of the feature vector is reduced while the information significance is preserved. The direction of the largest variance can be obtained by finding the eigenvector which corresponds to the largest eigenvalues [35]. The demonstration of PCA analysis is shown in Figure 11:

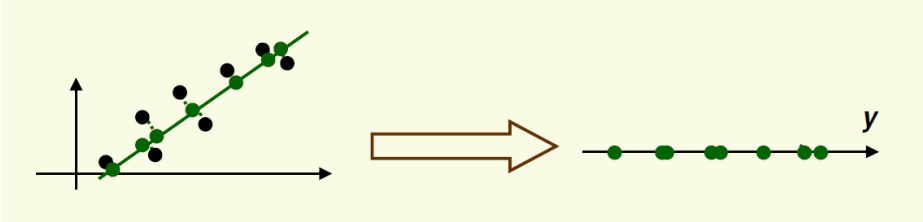

Figure 11: PCA component analysis [36]

When using the PCA technique both the training and testing samples will be processed using the same method illustrated below.

Assume that the training feature vector **X** has **m** vectors $\{x_1, x_2, \ldots, x_m\}^T$ with each feature vector x_i having a size **d**. Initially the sample mean is subtracted from the data as shown in the following equations.

$$z_i = (x_i - \mu) \tag{5}$$

where, the sample mean is defined as:

$$\mu = \frac{1}{m}\sum_{i=1}^{m} x_i \tag{6}$$

The sample size is reduced from dimension **d** to dimension **k** using a linear transformation. The linear transformation matrix **E** has size of **d×k** and it projects the sample vector $\boldsymbol{z_i}$ of size d to a reduced feature vector $\boldsymbol{y_i}$ of size **k**. The transformation matrix **E** is obtained from the eigenvectors of the scatter matrix **S** of the sample data $\boldsymbol{z_i}$. The following equations illustrate the derivation process.

$$y_i = z_i\, E \quad where\ i = 1,2, \ldots, m \tag{7}$$

The data scatter matrix is defined as:

$$S = \sum_{i=1}^{m} z^T{}_i z_i \tag{8}$$

The scatter of all projected samples is maximized by taking the eigenvectors which correspond to the **k** largest eigenvalues. Hence, the transformation matrix **E** can be expressed as:

$$E = [e1\ e2 \ldots ek] \tag{9}$$

where $\{ei|i = 1,2, \dots, k\}$ represents the eigenvectors which represent the **k** largest eigenvalues of the scatter matrix.

4.4.3 Classification Techniques

4.4.3.1 K-Nearest Neighbor Classifier (KNN)

The K-Nearest Neighbor Classifier or KNN classifier is one of the most simple and effective classification methods that could be applied. The KNN classification is non-parametric technique that can classify data which don't possess a well know distribution, like conventional linear, quadratic or Gaussian distributions. The KNN works by comparing each incoming test data point with the whole training data samples and then classify the data based on the nearest neighboring training samples. The KNN simply compares the distance between the testing samples and the **k** nearest samples, and then assigns the class depending on the nearest neighbors [38]. There are two main parameters which are required to design the KNN classifiers which are:

1. The value of ***K*** which decides the number neighboring samples which will be compared with the
2. The distance measure which decides how the distance between the test and training samples should be evaluated

There are several distance measures which can be used for the KNN classification including distance correlation, Euclidian distance, city-block and cosine distance.

1. Distance Correlation

Typically if the correlation between two data points is equal to zero, then the two points are independent. However, if the correlation is equal to 1 then the two points are dependent, implying that they come from the same class. The formulation for distance correlation is shown below:

$$dCor(x_g, y_p) = \frac{dCov(x_g, y_p)}{\sqrt{dVar(x_g) dVar(y_p)'}} \quad (10)$$

Or

$$dCor(x_g, y_p) = \frac{(x_g - \bar{x}_g)(y_p - \bar{y}_p)}{\sqrt{(x_g - \bar{x}_g)(x_g - \bar{x}_g)'}\sqrt{(y_p - \bar{y}_p)(y_p - \bar{y}_p)'}} \quad (11)$$

where,

$$\bar{x}_g = \frac{1}{n}\sum_j x_{g_j} \quad (12)$$

$$\bar{y}_p = \frac{1}{n}\sum_j y_{p_j} \quad (13)$$

Properties of distance correlation:

i. $0 \leq dCor(x_g, y_p) \leq 1$.

ii. $dCor(x_g, y_p) = 0$ if and only if x_g and y_p are independent.

iii. If $dCor(x_g, y_p) = 1$, then x_g and y_p are completely dependent.

In order to be used for KNN Classification the distance correlation is modified so that independent data should have a correlation distance of 1 and dependent data should have a correlation distance of 0. Therefore, the distance correlation can be modified as follows:

$$dCor(x_g, y_p)_s = 1 - \frac{(x_g - \bar{x}_g)(y_p - \bar{y}_p)}{\sqrt{(x_g - \bar{x}_g)(x_g - \bar{x}_g)'}\sqrt{(y_p - \bar{y}_p)(y_p - \bar{y}_p)'}} \quad (14)$$

For instance, if $dCor(x_g, y_p) = 0$, implying that x_g and y_p are independent, then the distance $dCor(x_g, y_p)_s$ is equal to 1. This indicates that the distance between x_g and y_p is very large and the chance that they are of the same class is very low. Similarly, For instance, if $dCor(x_g, y_p) = 1$, implying that x_g and y_p are dependent, then the distance $dCor(x_g, y_p)_s$ is equal to 0. This indicates that the distance between x_g and y_p is very small and the chance that they are of the same class is very high.

2. Euclidian Distance

The Euclidean distance is similar to the Pythagorean distance measure which can be formulated as:

$$d(x_g, y_p) = \sqrt{\sum_{k=1}^{d} \left(x_g^{(\kappa)} - y_p^{(\kappa)}\right)^2} \quad (15)$$

3. City Block Distance

The Cityblock or Manhattan distance approximates the Euclidean distance by the following formulation:

$$d(x_g, y_p) = \sum_{k=1}^{d} \left| x_g^{(\kappa)} - y_p^{(\kappa)} \right| \quad (16)$$

4. Cosine Distance

The cosine distance is evaluated by finding inner product between two vectors. In that sense the similarity between both vectors is measured. The cosine distance formula is shown below:

$$d(x_g, y_p) = \frac{x_g^T . y_p}{\|x_g\| \|y_p\|} \quad (17)$$

After the distance measure and **k** are selected, the KNN works by applying the following procedure. Given a training data set ***D*** and a test sample $z = (\tilde{x}_i, \tilde{y}_i)$, the KNN algorithm calculates the distances between the test point and all training points $(x, y) \in D$ to determine its nearest neighbor list, D_z, where:

- $\tilde{x}_i$ is the test data while $\tilde{y}_i$ is its class
- x is the training data set and *y* is the corresponding class set.

The test data is classified based on the majority class of its nearest neighbors as follows: First, $d(\tilde{x}_i, x)$or the distance between the testing data z and each training sample $(x, y) \in D$ is calculated. After that, $D_z \subseteq D$, the set of the closest ***K*** training objects to z will be selected. Finally**,** the algorithm will calculate the class $\tilde{y}$ of each testing data as:

$$\tilde{y} = (\arg max)_v \sum_{(x_i, y_i) \in D_z} I(v = y_i) \quad (18)$$

4.4.3.2 Polynomial Classifier

The polynomial classifier can be considered as an approximation to the optimal Bayes classifier. The classifier expands an incoming feature vector by adding

all pairwise products of the individual elements [39]. For example, a quadratic expansion for **X** containing 2-dimensional training feature vectors of different classes can be expressed as:

$$X = \begin{bmatrix} x_{11} & x_{12} \\ x_{21} & x_{22} \\ x_{31} & x_{32} \end{bmatrix} \tag{19}$$

Hence the augmented features are defined as

$$\mathbf{X_{aug}} = \begin{bmatrix} 1 & x_{11} & x_{12} & x_{11}x_{12} & x_{11}^2 & x_{12}^2 \\ 1 & x_{21} & x_{22} & x_{21}x_{22} & x_{21}^2 & x_{22}^2 \\ 1 & x_{33} & x_{32} & x_{31}x_{32} & x_{31}^2 & x_{32}^2 \end{bmatrix} \tag{20}$$

Assuming each row of **X** corresponds to a different ESDD value, the target matrix would be the output ESDD value. The weight matrix **W** is achieved by multiplying the Pseudo-inverse of $\mathbf{X_{aug}}$ by the target matrix.

$$W = Pinv\left(X_{aug}\right) B \tag{21}$$

Each incoming test feature vector **Y** has to undergo the same expansion of the training data. The class label of the test vector is then determined using the obtained weight matrix as follows:

$$C = {Y_{aug}}^T W \tag{22}$$

4.4.3.3 Neuro-Fuzzy logic

The idea of fuzzy logic was first introduced in 1965 to process data which have statistical uncertainties. The main concept for fuzzy logic is to work with approximate reasoning instead of exact reasoning. Therefore, the fuzzy logic could achieve better performance when the system has uncertainties. The approximate reasoning can be more suitable for systems which cannot be mathematically modeled. The fuzzy logic system has some limitations including the imprecision of the type, location and number of its membership functions. Neural networks, on the other hand, have the advantage of recognizing patterns by adjusting their weights. However, the learning process of neural networks is very slow as they keep updating the weights in order to be trained [40].

A hybrid neuro-fuzzy system takes advantage of both neural networks and fuzzy logic. The neural network will be used to tune the membership functions of

fuzzy systems which will increase the precision of fuzzy logic to represent uncertain statistical data. A typical fuzzy inference system has four main functions which are illustrated in the figure below:

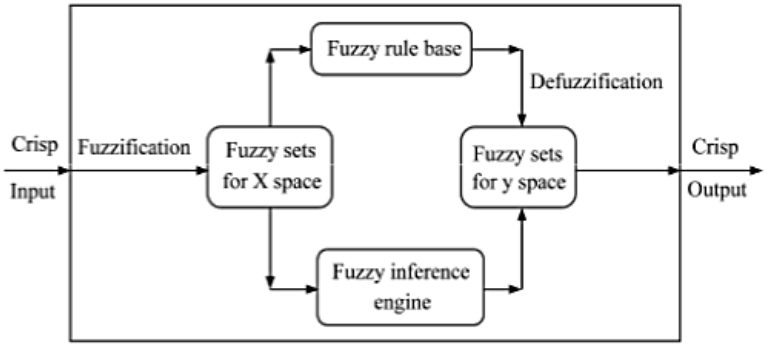

Figure 12: Fuzzy Inference System Main Blocks [40]

The first block corresponds to a knowledge base, which defines the fuzzy rules and database. These rules determine the membership functions in terms of their type. There are several types of membership functions including generalized bell, triangular, trapezoidal and sigmoid functions which are depicted in equations 23-26 respectively.

1. Generalized Bell Function:

$$f(x; a, b, c) = \frac{1}{1+\left|\frac{x-c}{a}\right|^{2b}} \tag{23}$$

where,

a determines the half width

b and a determine the slopes at the crossover points

c determines the center of the corresponding membership function

2. Triangular Function:

$$f(x; a, b, c) = \max\left(\min\left(\frac{x-a}{b-a}, \frac{c-x}{c-b}\right), 0\right) \tag{24}$$

Where,

a and *c* determine the lower points of the triangle

b determines the peak of the triangle

3. Trapezoidal Function:

$$f(x; a, b, c, d) = \max\left(\min\left(\frac{x-a}{b-a}, 1, \frac{d-x}{d-c}\right), 0\right) \quad (25)$$

where,

a and *d* determine the lower points of the trapezoid

b and *c* determine the upper points of the trapezoid

4. Sigmoid Function:

$$f(x; a, b) = \frac{1}{1+ e^{-ax}} \quad (26)$$

where,

a determine the slope

The inference engine is responsible for processing the inference operations on the rules. The fuzzification interface will find the degree of match between the input and their linguistic value, represented by the membership function. Finally at the defuzzification phase, the fuzzy result will be transformed back into its crisp output value.

The structure of an adaptive neuro fuzzy inference system is shown in Figure 13. In this model, X1 and X2 are the input data. Ai and Bi represents the input membership function. The output of the first layer represents the degree of matching between the input and the membership function (fuzzification). At the second layer, the combinations of degrees of match between different inputs are used to create the output signal. This signal represents the firing strength of the fuzzy rule for each association. At layer three, the firing strength of layer 2 outputs are normalized and fed to layer four. An output membership function will be used to derive the inferred output (Defuzzification). Finally at layer five, both inferred outputs will be used to calculate the output results.

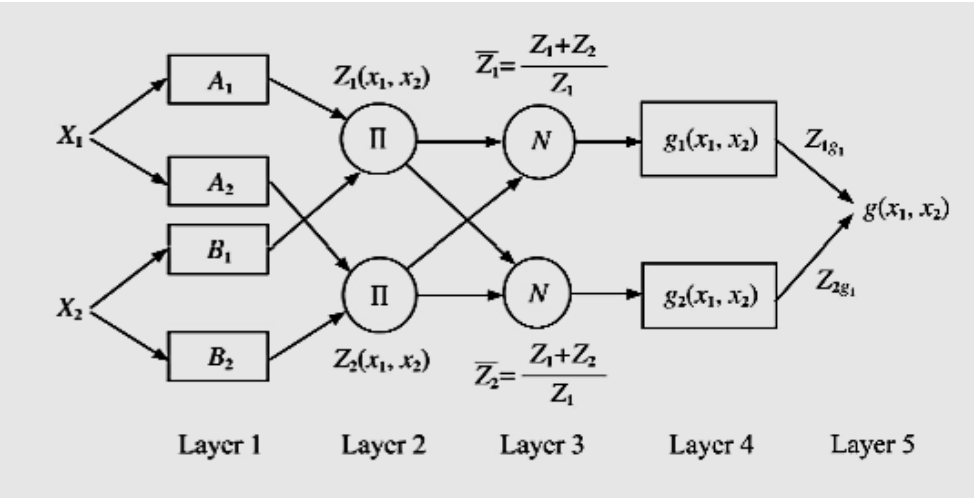

Figure 13: Two Input Adaptive Neuro Fuzzy Inference System Model [40]

Chapter 5: Results

5.1 Feature Selection and Reduction

The experimental procedure described in section four was performed 20 times using 4 insulators creating 80 data sets. The experiment time is 5 hours and the leakage current value was recorded every 10 seconds. For each experiment, the ESDD was measured at the end of the test and different features from the leakage current were calculated. These features include the peak value, fundamental, third and the fifth harmonic components. Each feature vector contains 1800 data points. A typical peak value of the leakage current during the test duration is depicted in Figure 14.

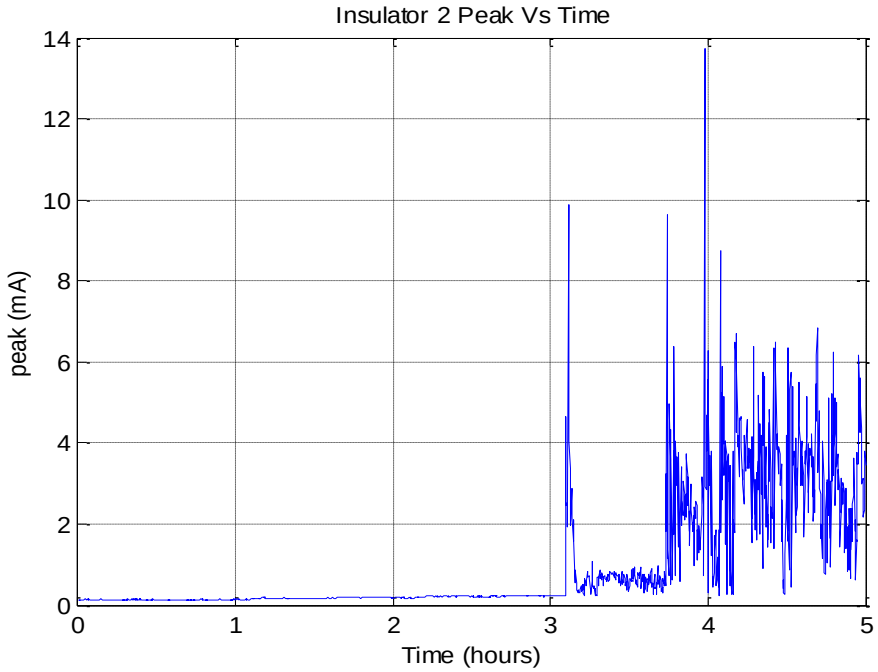

Figure 14: Peak Value of Leakage Current for 6 cm insulator tested at 0.3 kV/cm with a fog conductivity of 15 mS/cm

The LC features along with the experimental conditions were used for predicting the ESDD level. The experimental conditions include voltage stress, salt-fog conductivity and the insulator length. After combining all the features and the experimental conditions the best features that were selected are:

1. Voltage Stress
2. Salt-fog Conductivity
3. Insulator Length
4. LC average Peak Value for 5 hours
5. LC average peak value for each 15 minutes

6. Rate of change of LC average peak value
7. Rate of change of LC peak value

Two feature reduction techniques were used, which are stepwise regression and principle component analysis (PCA). While the stepwise regression technique chooses the best feature combinations, the PCA reduces the dimensionality of the feature vector by taking a linear combination of all features. The PCA reduced the dimensionality of the seven features mentioned above. However, the stepwise regression selected the following features:

1. Voltage Stress
2. Salt-fog Conductivity
3. Insulator Length
4. LC average Peak Value for 5 hours
5. LC average peak value for each 15 minutes

After feature reduction, the ESDD was predicted using KNN, Polynomial and Neuro-fuzzy classifiers. In addition, the prediction was performed using leave one out strategy.

5.2 ESDD Regression Analysis

Using leave-one out strategy, the 80 ESDD levels were predicted using the Stepwise regression and PCA combined with KNN, Polynomial and Neuro-fuzzy. The parameters for the classifiers were determined by trial and error. For KNN the distance measure which produced the maximum recognition rate was the correlation distance and the value of the constant *k* (number of neighbors) was 2. For the ANFIS model the membership function which gave the best recognition rates is the generalized bell function, while the number of membership function was 3.

The root mean square error (RMSE) was calculated to indicate the accuracy of the results. The RMSE is evaluated by the following formula.

$$\text{RMSE} = \sqrt{\frac{\sum_{i=1}^{n} (\hat{y}_t - y_t)^2}{n}} \tag{27}$$

where,

$\hat{y}_t$ represents the predicted value

y_t represents the actual value

In addition, the recognition rate was also measured for each classifier. Finally, the classifier results were combined by taking an average value for the three

classifiers which were used. The classifier fusion was done at the score level by averaging the predicted ESDD level of the three classifiers. The results of the regression analysis are presented in Table 6.

Table 6 Regression Analysis Results

Reduction Technique	Classifier	Recognition Rate	RMSE Error
Step-wise Regression	KNN	**64.4 %**	**0.0360**
	Polynomial	**62.2 %**	**0.0427**
	ANFIS	**48.4 %**	**0.0595**
	Combined Classifiers	**67.3 %**	**0.0321**
PCA	KNN	**59.5 %**	**0.0509**
	Polynomial	**63.1 %**	**0.0327**
	ANFIS	**52.6 %**	**0.0477**
	Combined Classifiers	**66.7 %**	**0.0320**

Table 6 shows that the best RMSE values for PCA and Step-wise regression are 0.0320 and 0.0321 respectively. These values are close to several results in the literature. For instance, the RMSE error was 0.0407 in [29], 0.0252 in [32] and the average absolute difference was 0.035 in [31]. Also, the maximum recognition rate is 67.3 % for Step-wise regression and 66.7 % for PCA analysis. The main possible reason for this low rate is the unaccounted effect of hydrophobicity and fluid migration which influences the development of leakage current. The hydrophobic behavior of polymer insulators arises due to the low surface energy on its surface. This property allows the insulator to resist the aging process and pollution deposition. In addition, low molecular fluids migrate to the surface and enhance the hydrophobic abilities of the insulator and it is difficult to measure the low molecular content. The prediction of ESDD level for ceramic insulation is more straightforward as it has no hydrophobic properties or low molecular fluid reserve. Stem plots for the regression analysis are shown in Figures 15 - 20.

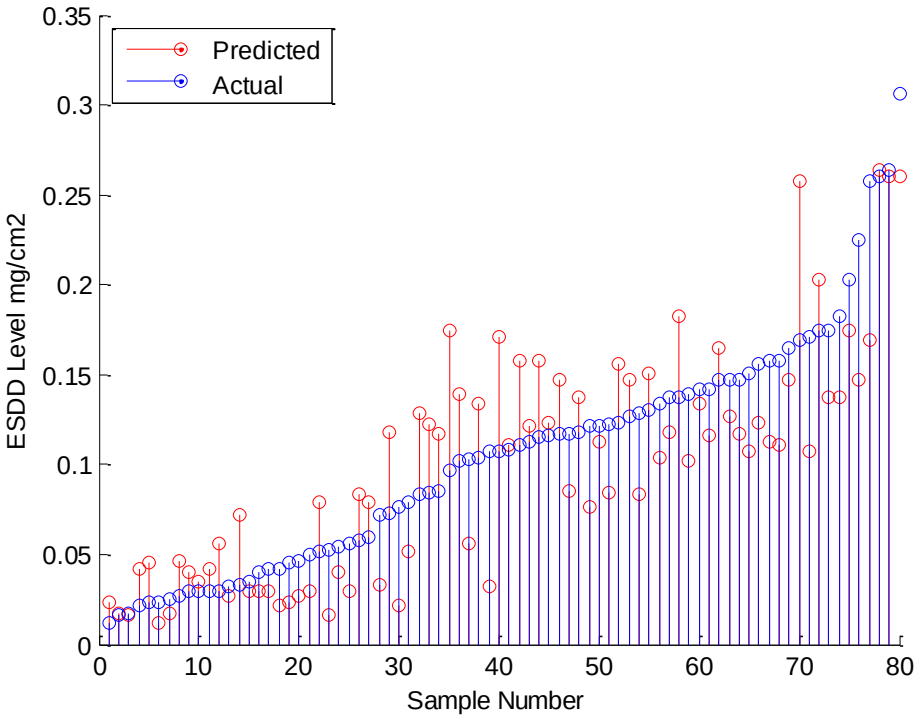

Figure 15: Regression Results for Stepwise analysis and KNN Classifier

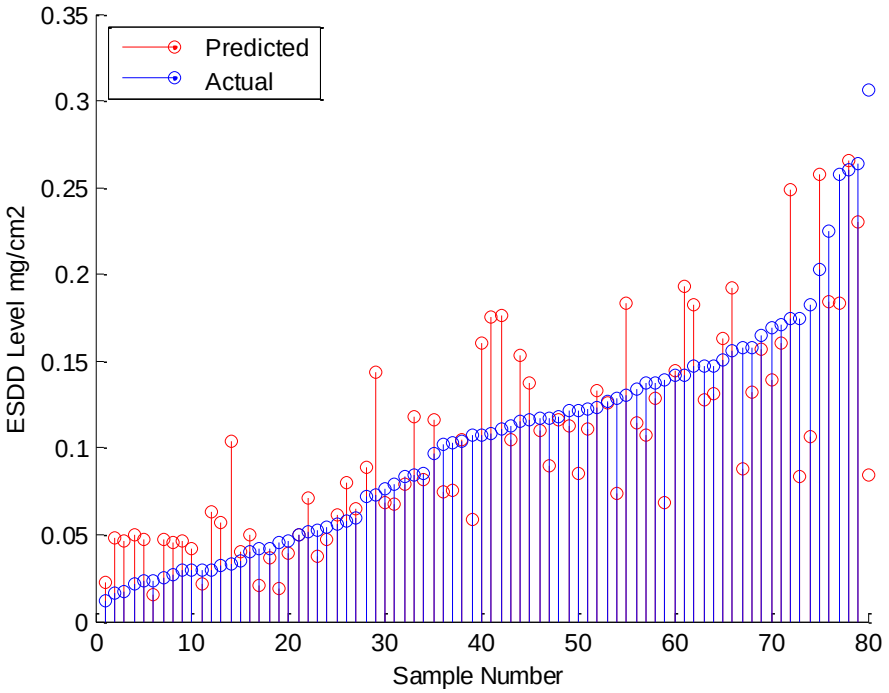

Figure 16: Regression Results for Stepwise analysis and Polynomial Classifier

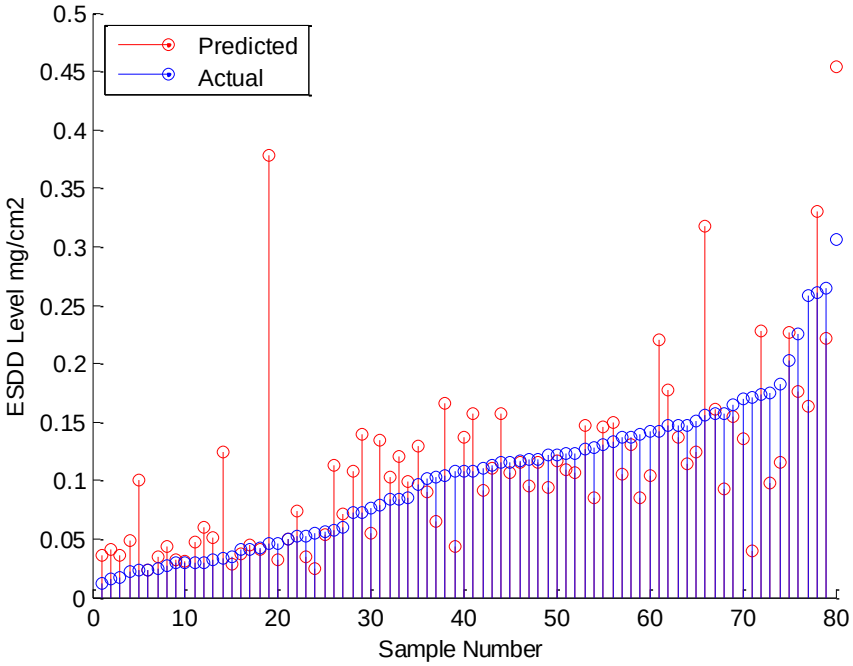

Figure 17: Regression Results for Stepwise analysis and ANFIS Classifier

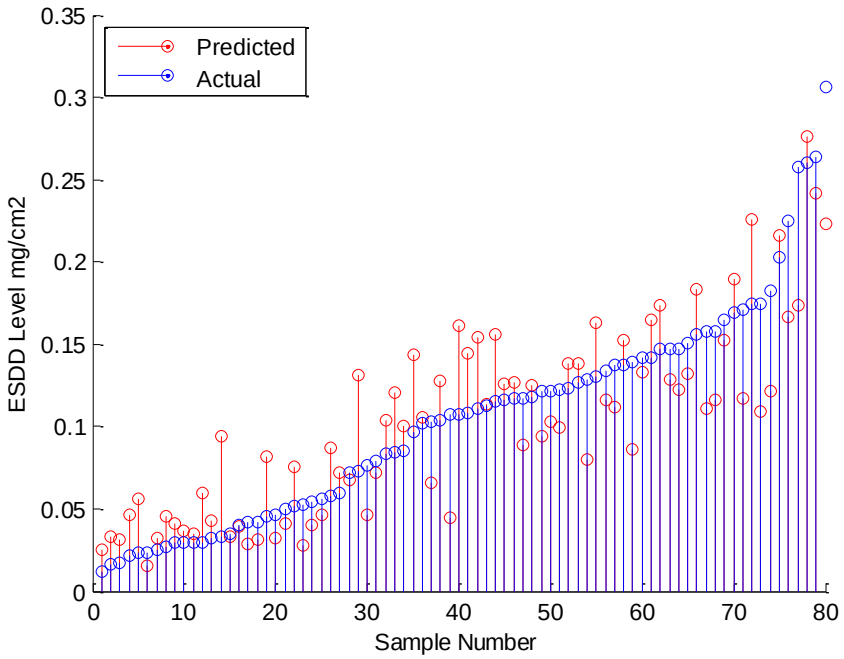

Figure 18: Regression Results for Stepwise analysis and Combined Classifiers

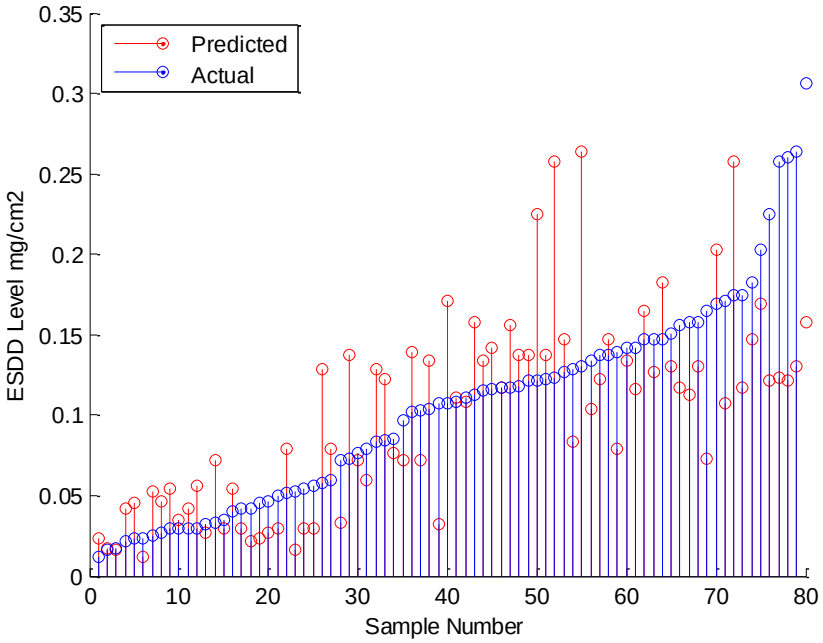

Figure 19: Regression Results for PCA analysis and KNN Classifier

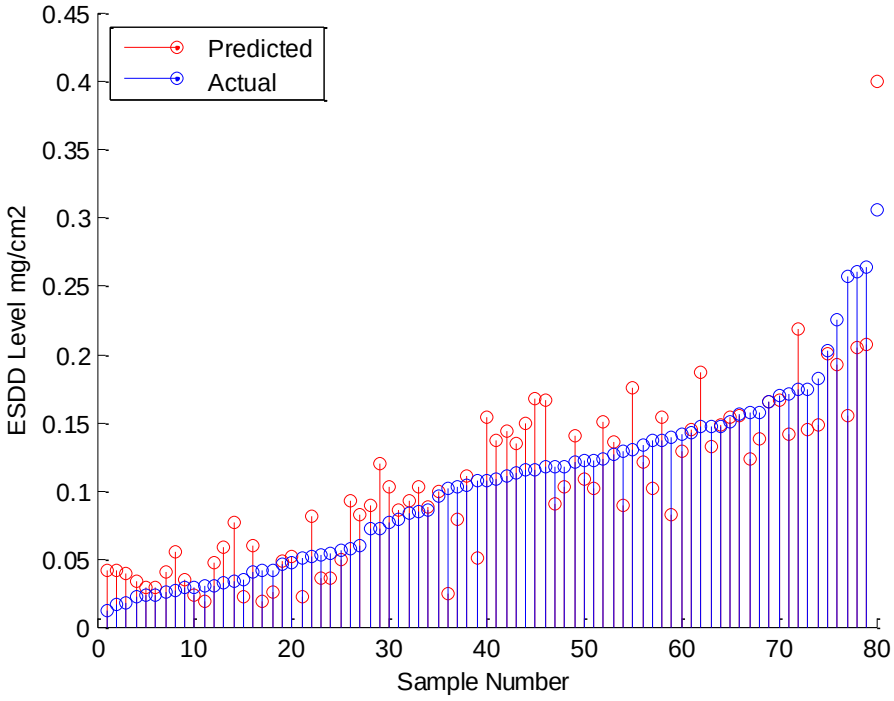

Figure 20: Regression Results for PCA analysis and Polynomial Classifier

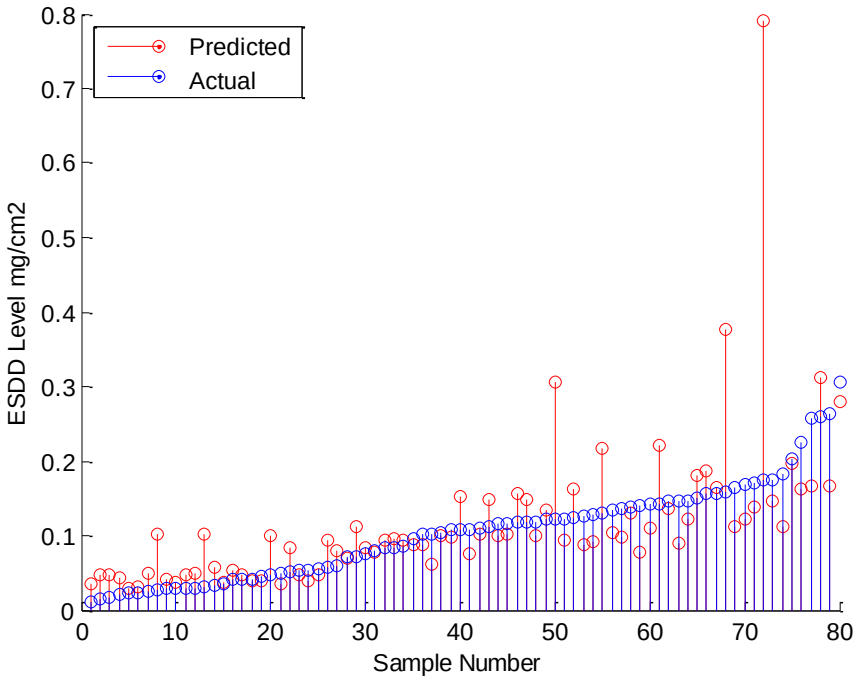

Figure 21: Regression Results for PCA analysis and ANFIS Classifier

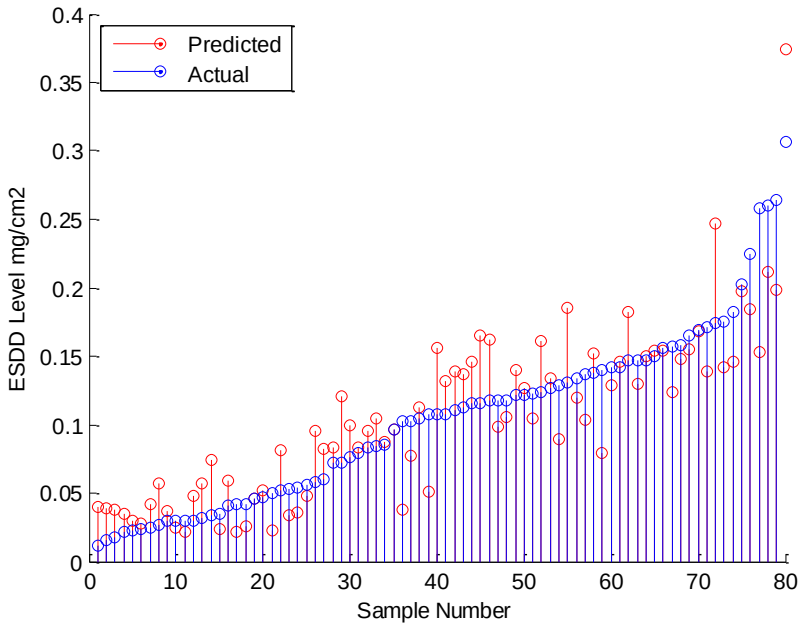

Figure 22: Regression Results for PCA analysis and Combined Classifiers

Alternatively, instead of predicting the actual level of the ESDD, the ability to predict the range of ESDD value will be investigated. According to IEC 60587 standards, the ESDD ranges that reflect the surface condition of the insulator are shown in Table 7.

Table 7: ESDD Range and Surface Contamination Severity

ESDD Range (mg/cm2)	Contamination Severity Classification
0 - 0.03	Clean or Very Light
0.03 - 0.06	Light
0.06 -0.1	Moderate
> 0.1	Heavy

Therefore, the prediction problem was modified to predict the range of ESDD level or the surface contamination severity.

5.3 Contamination Level Class Prediction

Instead of finding the actual value of the ESDD level, the contamination severity class will be evaluated by predicting the ESDD range. The contamination class reflects a practical indication of the surface condition of the insulator.

5.3.1 Four Class Prediction

The pollution severity classes according to the IEC 60587 standard were converted into a four class problem as shown in Table 8:

Table 8: Four Class Prediction

ESDD Range (mg/cm2)	Contamination Severity Classification	Class	Number of Data Points
0 - 0.03	Clean or Very Light	1	12
0.03 - 0.06	Light	2	14
0.06 -0.1	Moderate	3	9
> 0.1	Heavy	4	45

The data points for class 1, 2, and 3 are relatively low compared to class 4. The aging process for polymer insulator is stochastic in nature, meaning that the same conditions may result in different behavior. For this reason, it is hard to control the outcome of the experiment in order to generate balanced data set among the four ESDD classes. For instance it is relatively easy to conduct the experiment to have very high ESDD level. However, it is very hard to control the experiment output to produce results in the lower and middle ranges of ESDD level. This may create a

problem as the classifiers will be more biased towards class 4. To minimize this effect, the classifiers will be used as "regressors" to predict the actual ESDD value, and then the range of ESDD will be assigned depending on the predicted ESDD value.

Using leave one out strategy, the 80 ESDD levels were predicted using stepwise regression and PCA analysis combined with KNN, Polynomial and Neuro-fuzzy Classifiers. Table 9 summarizes the results for the four class classification problem.

Table 9: Summary of Four Class Prediction Results

Reduction Technique	**Classifier**	**Recognition Rate**				
		Class 1	**Class 2**	**Class 3**	**Class 4**	**Total**
Step-wise Regression	KNN	42 %	7 %	11 %	87 %	**57.5 %**
	Polynomial	25 %	57 %	67 %	78%	**65 %**
	Neuro-fuzzy	8 %	57 %	22%	76%	**56.25 %**
	Combined Classifiers	25%	71 %	67%	80%	**68.75 %**
PCA	KNN	33%	7 %	56%	89%	**62.5 %**
	Polynomial	33%	59 %	67%	87%	**70 %**
	Neuro-fuzzy	8%	71 %	89%	78%	**67.5 %**
	Combined Classifiers	33%	50 %	78%	89%	**72.5 %**

The PCA reduction has a higher overall recognition rates compared to the step-wise regression. The maximum overall recognition rate is 72.5 % for polynomial classifier and PCA analysis. However, classes 1, 2 and 3 suffer from relatively low recognition rate due to the low available number of data points. To improve further the classification rate, both class 1 and 2 will be combined together. The rational of such combination can be explained as follows: the distinction between class 1 (Clean or very light contamination) and class 2 (light contamination) will not have a significant practical impact when it comes to maintenance or cleaning routines.

5.3.2 Three Class Prediction

The first two classes of the IEC 60587 standard were combined to form a single class. This resulted in a 3 class classification problem as shown in Table 10:

Table 10: Three Class Prediction

ESDD Range (mg/cm2)	Contamination Severity Classification	Class	Number of Data Points
0 - 0.06	Clean or Light	1	26
0.06 -0.1	Moderate	2	9
> 0.1	Heavy	3	45

The number of class 1 has increased, which will create a more balanced classification problem. Using leave one out strategy the 80 ESDD levels were predicted using stepwise regression and PCA analysis combined with KNN, Polynomial and Neuro-fuzzy Classifiers. Table 11 summarizes the results for the three class classification:

Table 11: Summary of Three Class Prediction Results

Reduction Technique	**Classifier**	**Recognition Rate**			
		Class 1	**Class 2**	**Class 3**	**Total**
Step-wise Regression	KNN	88 %	11 %	87 %	**78.6 %**
	Polynomial	81 %	67 %	78 %	**77.5 %**
	Neuro-fuzzy	81 %	22 %	76 %	**71.25 %**
	Combined Classifiers	85 %	67 %	80 %	**80 %**
PCA	KNN	88%	56 %	89 %	**85 %**
	Polynomial	88%	67%	87%	**85 %**
	Neuro-fuzzy	81%	89 %	78 %	**80 %**
	Combined Classifiers	88 %	78 %	89 %	**87.5 %**

Compared to step-wise regression, the PCA technique has resulted in a relatively better recognition for all classes. The KNN and Polynomial recognition rates increased from around 78 % to 85 %. The Neuro-fuzzy classifier has improved from 71.25 % to 80%. The PCA also improved the results for the four class problem.

It can be concluded that the PCA is a better reduction technique than the stepwise regression. In the three class problem the recognition rates were higher compared to the four class problem as the number of cases for class 1 has increased. This created a more balanced recognition problem which improved the overall recognition.

Followed by PCA, the KNN and polynomial classifiers achieved the highest recognition rates of 85%, while the Neuro-fuzzy classifier achieved the lowest rate of 80%. However, The KNN and polynomial classifiers were not able to recognize class 2 with high accuracy. On the other hand, the Neuro-fuzzy classifier was able to recognize class 2 with a very good accuracy of 89%. Therefore, taking an average of the three classifiers could increase the recognition rate of class 2 and maintain a high overall recognition rate. Taking an average value for KNN, polynomial and neuro-fuzzy classifiers produced the highest recognition rate of 87.5 %. In addition, the classification rate for class 2 is around 78%. Therefore, combining the results of the classifiers improved the overall recognition rates and maintained a good accuracy for class 2.

5.3.3 Two Class Prediction

To further increase the number of data points for each class, the first two classes of the IEC 60587 standard were combined to form class 1 and the last two classes were combined to form class 2. This resulted in a 2 class classification problem as represented in Table 12:

Table 12: Two Class Prediction

ESDD Range (mg/cm2)	Contamination Severity Classification	Class
0 - 0.06	Clean or Light	1
> 0.06	Moderate or Heavy	2

As previously reported, the PCA analysis proved to be better than stepwise regression when it comes to feature reduction therefore; it is used for the 2-class prediction. The prediction was done using leave one out strategy and applying KNN, Polynomial and Neuro-Fuzzy and the results are depicted in Table 13.

All classifiers had high recognition rates of 93.75%. The KNN and Polynomial Classifiers achieved similar results and they predicted both classes with high accuracy. The neuro-fuzzy classifier predicted class 1 with less precision than

the KNN and the polynomial classifier, however; it predicted class 2 with higher precision. When the classifiers were combined, the recognition rate increased to 95% and the recognition rates for classes 1 and 2 are both above 90%. Such increase in the recognition rate demonstrates the importance of increasing the number of data point per class. Therefore, the proposed technique has the potential to be used in the field to predict the ESDD class if the number of the data point is sufficient in each class.

Table 13: Summary of Two Class Prediction Results

Classifier	**Recognition Rate**		
	Class 1	**Class 2**	**Total**
KNN	88 %	96 %	**93.75 %**
Polynomial	88 %	96 %	**93.75 %**
Neuro-fuzzy	81 %	100 %	**93.75 %**
Combined Classifiers	92 %	96 %	**95 %**

Chapter 6: Conclusions and Recommendations

6.1 Conclusions

Polymer outdoor insulators are becoming more popular due to their low cost, light weight and pollution resistance property known as hydrophobicity. However, the mechanism of hydrophobicity is still not fully understood. Many researches have been done on polymer insulators to monitor or predict their aging process using the leakage current. Unlike ceramic and porcelain, little work has been done to predict the ESDD level or pollution severity on the surface of polymer insulators. In this study, the surface severity class of polymer outdoor insulation was predicted using leakage current monitoring and ESDD level prediction.

Two reduction techniques were used for the prediction, which are the stepwise regression and PCA analysis. Three classifiers were used including KNN, polynomial and Neuro-fuzzy classifiers. The PCA performed better the stepwise regression in all classification cases. The actual value of ESDD level was predicted with nearly 60% recognition rate for all classifiers. Despite this low recognition rate, the surface condition was evaluated using the IEC standard pollution level classification. Instead of finding the actual ESDD value, the pollution level was classified according to the ESDD range. Creating a four class problem resulted in a low recognition rates using the stepwise regression. The best recognition rate was 65%. Using PCA analysis the recognition rate reached up to 70%. The reason for this problem is the relatively small number of classes 1, 2 and 3 compared to class 4.

By combining classes 1 and 2 together, the classification problem was turned into a three class problem. Combining the first 2 classes does not have a significant impact on the practicality of the classification. Class 1 represents clean and very light contamination levels, while class two represents light contamination level. The recognition rates using PCA increased up to 85% for the KNN and Polynomial classifiers. However, both classifiers achieved low recognition rates for class 2, which is relatively small compared to classes 1 and 3. The neuro-fuzzy classifier achieved 80% recognition rate and was able to achieve high recognition rate for class 2. Taking a combination of the three classifiers increased the overall recognition rate up to 87.5% and the recognition rate for class two to almost 80 %.

The problem was further simplified to a 2 class problem by combining classes 1 and 2 into one class and classes 3 and 4 into a second class. The recognition rates

for all classifiers using PCA increased to 93.75 % with high recognition rates for both classes. It can be concluded that the leakage current can effectively predict 3 pollution severity classes for polymer insulation.

6.2 Future Work

This research study can be extended by trying to predict the non-soluble density deposit (NSDD) level for the polymer insulation. In addition, the effect of different environmental conditions, like temperature and humidity could be studied for polymer insulators. More features could be used in the prediction including the partial discharge. Also clean fog test could be used to predict the ESDD level and the test duration could be increased. Moreover, full length insulators could be used while keeping the insulator's shed. More importantly, this research methodology could be applied in the field on real insulators which will help in developing a reliable system for predicting the ESDD level and evaluating the surface condition of the insulators.

References

[1] R.S. Gorur, E.A. Cherney, and J.T. Burnham, Outdoor Insulators. Ravi S. Gorur Inc., 1999.

[2] E. Kuffel, W.S. Zaengl and J. Kuffel, High Voltage Engineering Fundamentals. Butterworth-Heinemann, 2000.

[3] J. P. Reynders, I. R. Jandrell, and S. M. Reynders, “Review of aging and recovery of silicone rubber insulation for outdoor use,” *IEEE Trans. on Dielectrics and Electrical Insulation*, vol. 6, no.5, pp. 620-631, 1999.

[4] H. Hillborg and U. W. Gedde, "Hydrophobicity Changes in Silicone Rubbers," *IEEE Trans. on Dielectrics and Electrical Insulation*, Vol. 6, no.5, pp. 703-717, 1999.

[5] M. Ali, R. Hackam, "Effects of saline water and temperature on surface properties of HTV silicone rubber," *IEEE Trans. on Dielectrics and Electrical Insulation*, vol.15, no.5, pp.1368-1378, Oct 2008.

[6] N. Yoshimura, S. Kumagai, and S. Nishimura, “Electrical and environmental aging of silicone rubber used in outdoor insulation,” *IEEE Trans. on Dielectrics and Electrical Insulation*, vol. 6, no.5, pp. 632-650, 1999.

[7] I.J.S. Lopes, S.H. Jayaram, E.A. Cherney, "A method for detecting the transition from corona from water droplets to dry-band arcing on silicone rubber insulators," *IEEE Trans. on Dielectrics and Electrical Insulation*, vol.9, no.6, pp.964-971, Dec 2002.

[8] M.A.R.M. Fernando, S.M. Gubanski, “Leakage current patterns on contaminated polymeric surfaces,” *IEEE Trans. on Dielectrics and Electrical Insulation*, vol.6, no.5, pp.688-694, Oct 1999.

[9] T. Suda, “Frequency characteristics of leakage current waveforms of an artificially polluted suspension insulator,” *IEEE Trans. on Dielectrics and Electrical Insulation*, vol.8, no.4, pp.705-709, Aug 2001.

[10] A.H. El-Hag, S.H. Jayaram, E.A. Cherney, “Fundamental and low frequency harmonic components of leakage current as a diagnostic tool to study aging of RTV and HTV silicone rubber in salt-fog,” *IEEE Trans. on Dielectrics and Electrical Insulation*, vol.10, no.1, pp.128-136, Feb 2003.

[11] M.A.R. Fernando and S.M. Gubanski, “leakage Current on Non-ceramic Insulators and Materials," *IEEE Trans. on Dielectrics and Electrical Insulation*, vol. 6, no.5, pp. 660-667, Oct 1999.

[12] R.Barsch, H. Jahn, J. Lambrecht and F. Schmuck, "Test methods for polymeric insulating materials for outdoor HV insulation," *IEEE Trans. on Dielectrics and Electrical Insulation*, vol.6, no.5, pp.668-675, Oct 1999.

[13] S.Venkataraman and R.S. Gorur, "Prediction of flashover voltage of non-ceramic insulators under contaminated conditions," *IEEE Trans. on Dielectrics and Electrical Insulation*, vol.13, no.4, pp.862-869, Aug 2006.

[14] S. Chandrasekar, K. Krishnamoorthi, M. Panneerselvam and C.Kalaivanan, ''Investigations on Flashover Performance of Porcelain Insulators under Contaminated Conditions,'' National Conf. Electrical Engineering and Embedded Systems, (NCEEE), pp.112-116, 2008.

[15] V. T. Kontargyri , A. A. Gialketsi , G. J. Tsekouras , I. F. Gonos and I. A. Stathopulos "Design of an artificial neural network for the estimation of the flashover voltage on insulators", *Electr. Power Syst. Res.*, vol. 77, pp.1532-1540, 2007.

[16] P. S. Ghosh, S. Chakravorti and Chatterjee, "Estimation of Time to Flashover Characteristics of Contaminated Electrolytic Surfaces Using Artificial Neural Network," *IEEE Trans. On Dielectric and Electrical Insulation*, Vol.2, pp.1064-1074, 1995.

[17] P. Cline , W. Lannes and G. Richards "Use of pollution monitors with a neural network to predict insulator flashover", *Electric Power Systems Research*, no. 42, pp.27-33, 1997

[18] IEEE Standard Techniques for High-Voltage Testing," IEEE Std 4-1995, pp.1-135, Oct 1995.

[19] Jingyan Li, Wenxia Sima, Caixin Sun and Sebo, S.A.; , "Use of leakage currents of insulators to determine the stage characteristics of the flashover process and contamination level prediction," *IEEE Trans. on Dielectrics and Electrical Insulation*, vol.17, no.2, pp.490-501, April 2010.

[20] I.A. Joneidi, J. Jadidian, R. Karimpour, A.A. Shayegani and H. Mohseni, "Effects of ultraviolet radiation and artificial pollution on the leakage current of Silicon Rubber insulators," IEEE Electr.Insul. Conf. (EIC), pp.304-308, 2011.

[21] A.N. Jahromi, A.H. El-Hag, E.A. Cherney, S.H. Jayaram, M. Sanaye-Pasand and H. Mohseni, "Prediction of leakage current of composite insulators in salt fog test using neural network," Electrical Insulation and Dielectric Phenomena. Annual Report Conference on CEIDP, pp. 309-312, 16-19 Oct 2005.

[22] A.H. El-Hag, A.N. Jahromi and M. Sanaye-Pasand, “Prediction of Leakage Current of Non-ceramic Insulators in Early Aging Period,” *Electr. Power Syst. Res.*, vol.78, pp.1686-1692, 2008.

[23] C. Volat, F. Meghnefi, M. Farzaneh and H. Ezzaidi, "Monitoring leakage current of ice-covered station post insulators using artificial neural networks," *IEEE Transactions on Dielectrics and Electrical Insulation*, vol.17, no.2, pp.443-450, April 2010.

[24] Muhsin Tunay Gencoglu,Murat Uyar, "Prediction of flashover voltage of insulators using least squares support vector machines," *Expert Systems with Applications*, vol.36, pp.10789-10798, 2009.

[25] L. Nasrat and S. Aly, "Evaluation of Flashover Voltage on Hydrophobic Polymer Insulators with Artificial Neural Network," *International Journal of Electrical and Computer Engineering*, vol.2, no.4, pp. 487-494, Aug 2012.

[26] V. Kontargyri, G. Tsekouras, A. Gialketsi and P. Kontaxis, "Comparison between artificial neural networks algorithms for the estimation of the flashover voltage on insulators," International Conference on neural networks, May 2-4 2008.

[27] L. Maraaba, Z. Al-Hamouz and H. Al-Duwaish, "Estimation of high voltage insulator contamination using a combined image processing and artificial neural networks," IEEE 8th International Power Engineering and Optimization Conference (PEOCO), pp.214-219, 24-25 March 2014.

[28] R. de Aquino, J. Bezerra, M. Lira, G. Santos, O. Neto and C. de O.Lira, "Combining Artificial Neural Network for diagnosing polluted insulators," International Joint Conference on Neural Networks (IJCNN), pp.179-183, 14-19 June 2009.

[29] X. Jianyuan, S. Wei, C. Rong, T. Yun and L. Xin, "A new combination forecasting model for ESDD prediction of suspension porcelain insulators," 1st International Conference on Electric Power Equipment - Switching Technology (ICEPE-ST), pp.279-282, 23-27 Oct 2011.

[30] M. A. Salam, S. M. Al-Alawi, A. A. Maqrashi, "Prediction of Equivalent Salt Deposit Density of Contaminated Glass Plates Using Artificial Neural Networks," *Journal of Electrostatics, Elsevier Science*, Vol. 66, no.9-10, pp. 526-530, Sep 2008.

[31] J. Li, C. Sun, W. Sima, Q. Yang and Jianlin Hu, "Contamination Level Prediction of Insulators Based on the Characteristics of Leakage Current," *IEEE Trans. On Power Delivery*, vol.25, no.1, pp.417-424, Jan 2010.

[32] C. Muniraj and S. Chandrasekar, "Adaptive Neurofuzzy Inference System-Based Pollution Severity Prediction of Polymeric Insulators in Power Transmission Lines," *Advances in Artificial Neural Systems*, vol.2011, Article ID 431357, 9 pages, 2011.

[33] Electrical Insulating Materials Used under Severe Ambient Conditions Test Methods for Evaluating Resistance to Tracking and Erosion, IEC 60587 International Standard, 3"' ed., 2007.

[34] S. Hoda, G. Gopakumar and N.Mahdi, "Online Monitoring of Leakage Current in Outdoor Insulators," Senior Design Project, AUS, fall 2012.

[35] C. Bishop, "Pattern Recognition and Machine Learning," Springer Science, 2006.

[36] El Khatib, A.; Assaleh, K.; Mir, H., "Space-Time Adaptive Processing Using Pattern Classification," *IEEE Transactions on Signal Processing*, vol.63, no.3, pp.766-779, Feb 2015.

[37] G. Wang and C. Jain, Regression Analysis Modeling & Forecasting, Graceway Publishing Company, 2003.

[38] L. Kuncheva, Combining Pattern Classifiers: Methods and Algorithms, Wiley-Interscience, 2004.

[39] K. Assaleh and A. El-Hag, "Estimating transformer oil parameters using polynomial networks," International Conference on Condition Monitoring and Diagnosis (CMD), pp.1335-1338, 21-24 April 2008.

[40] S. Sabzi, P. Javadikia, H. Rabbani, A. Adelkhani and L. Naderloo, "Exploring the best model for sorting Blood orange using ANFIS method," *Agric Eng Int: CIGR Journal*, vol.15, no.4, Dec 2013.

[41] Ghunem, R.A.; Assaleh, K.; El-Hag, A.H., "Artificial neural networks with stepwise regression for predicting transformer oil furan content," *IEEE Transactions on Dielectrics and Electrical Insulation*, vol.19, no.2, pp.414-420, April 2012.

Vita

Abdelrahman Khaled joined the American University of Sharjah (AUS) in 2008 studying Electrical Engineering. He received his B.S. (cum laude) in Electrical Engineering from the AUS in fall 2011. During his study he concentrated on electric power distribution and protection. In spring 2012, he worked as a teacher assistant to pursue his M.S. degree in Electrical Engineering at AUS. During his graduate study he concentrated on high voltage engineering, power dispatch and pattern recognition. His preferred areas of study include power distribution and high voltage engineering.